

18 ARO 13031.3-MS

LEVEL IV

12

AD A 0 7 5 7 6 2

6

REACTION OF CALCIUM SILICATES WITH CARBON DIOXIDE AND WATER

DDC  
OCT 19 1979  
RECEIVED

9

FINAL REPORT, Jan 76 - Jan 79

10

J. Francis Berger  
R. L. Young  
Principal Investigators

11

26 Sept 1979

This document has been approved  
for public release and sale; its  
distribution is unlimited.

12 39

U. S. Army Research Office  
ARO Project Nos. 13031, 13031-MS  
Grants DAAG29-76-G-0016  
DAAG29-78-G-0049

DDC FILE COPY

Departments of Civil and Ceramic Engineering  
University of Illinois at Urbana-Champaign  
Urbana, Illinois 61801

79 10 19 159  
175-750

PII Redacted

12

REACTION OF CALCIUM SILICATES WITH CARBON DIOXIDE AND WATER

FINAL REPORT

PII Redacted

R. L. Berger  
J. F. Young  
Principal Investigators

DDC  
RECEIVED  
OCT 19 1979  
E

September 26, 1979

U. S. Army Research Office  
ARO Project Nos. 13031, 13031-MS  
Grants DAAG29-76-G-0016  
DAAG29-78-G-0049

Departments of Civil and Ceramic Engineering  
University of Illinois at Urbana-Champaign  
Urbana, Illinois 61801

This document has been approved  
for public release and sale; its  
distribution is unlimited.

Unclassified

SECURITY CLASSIFICATION OF THIS PAGE (When Data Entered)

| REPORT DOCUMENTATION PAGE   |                       | READ INSTRUCTIONS<br>BEFORE COMPLETING FORM                                    |
|---|-----------------------|--|
| 1. REPORT NUMBER<br><del>DRXRO PP L 13031 MS</del>  | 2. GOVT ACCESSION NO. | 3. RECIPIENT'S CATALOG NUMBER  |
| 4. TITLE (and Subtitle)<br>Reaction of Calcium Silicates with Carbon Dioxide and Water  |                       | 5. TYPE OF REPORT & PERIOD COVERED<br>FINAL<br>January 1976-January 1979       |
|   |                       | 6. PERFORMING ORG. REPORT NUMBER   |
| 7. AUTHOR(s)<br>R. Lee Berger<br>J. Francis Young   |                       | 8. CONTRACT OR GRANT NUMBER(s)<br>DAAG 29-76-G-0016<br>DAAG 29-67-G-0049<br>78 |
| 9. PERFORMING ORGANIZATION NAME AND ADDRESS<br>Departments of Civil & Ceramic Engineering<br>University of Illinois at Urbana-Champaign<br>Urbana, Illinois 61801   |                       | 10. PROGRAM ELEMENT, PROJECT, TASK AREA & WORK UNIT NUMBERS                    |
| 11. CONTROLLING OFFICE NAME AND ADDRESS<br>U. S. Army Research Office<br>P. O. Box 12211<br>Research Triangle Park, NC 27709  |                       | 12. REPORT DATE<br>26 September 1979   |
|   |                       | 13. NUMBER OF PAGES  |
| 14. MONITORING AGENCY NAME & ADDRESS (if different from Controlling Office)   |                       | 15. SECURITY CLASS. (of this report)<br><br>Unclassified                       |
|   |                       | 15a. DECLASSIFICATION/DOWNGRADING SCHEDULE                                     |
| 16. DISTRIBUTION STATEMENT (of this Report)<br><br>Approved for public release; distribution unlimited.   |                       |  |
| 17. DISTRIBUTION STATEMENT (of the abstract entered in Block 20, if different from Report)  |                       |  |
| 18. SUPPLEMENTARY NOTES<br>The view, opinions, and/or findings contained in this report are those of the author(s) and should not be construed as an official Department of the Army position, policy, or decision, unless so designated by other documentation.  |                       |  |
| 19. KEY WORDS (Continue on reverse side if necessary and identify by block number)<br>Ca <sub>3</sub> SiO <sub>5</sub> , β-Ca <sub>2</sub> SiO <sub>4</sub> , γ-Ca <sub>2</sub> SiO <sub>4</sub> , Ca <sub>3</sub> Si <sub>2</sub> O <sub>7</sub> , β-CaSiO <sub>3</sub> , silica gel, carbonation calcium silicate hydrate, kinetics, activation energy  |                       |  |
| 20. ABSTRACT (Continue on reverse side if necessary and identify by block number)<br>→ The reaction of five calcium silicates with CO <sub>2</sub> and water were investigated. The calcium silicates differed in Ca/Si ratio or polymorphic type. Reaction kinetics were dependent on the Ca/Si ratio of the initial calcium silicates. Activation energy for the carbonation reaction ranged from 9.8 kcal/mole for Ca <sub>3</sub> SiO <sub>5</sub> to 22.9 kcal/mole for CaSiO <sub>3</sub> . The reaction products were calcium carbonate (CaCO <sub>3</sub> ) and a calcium silicate hydrate of variable stoichiometry. The Ca and H <sub>2</sub> O content of the calcium silicate hydrate → |                       |  |

DD FORM 1 JAN 73 1473

EDITION OF 1 NOV 65 IS OBSOLETE

Unclassified

SECURITY CLASSIFICATION OF THIS PAGE (When Data Entered)

product decreases with degree of reaction. This results in the final stable reaction products consisting of calcium carbonate and a highly polymerized hydrous silica gel which is insoluble in HCl. Calcite forms during the carbonation of  $\text{Ca}_3\text{SiO}_5$ ,  $\beta\text{-Ca}_2\text{SiO}_4$ , and  $\gamma\text{-Ca}_2\text{SiO}_4$  if free water is present. Aragonite forms in the absence of free  $\text{H}_2\text{O}$  and in the carbonation of  $\text{CaSiO}_3$ . The carbonation reaction decreases rapidly at  $\text{CO}_2$  pressures  $< 0.12$ . At pressures from 0.12 to 54 atm the carbonation reaction increases, but at a slow rate. Temperature and relative humidity have significant influences on the rate of carbonation.

gamma

Beta

|                     |                                     |
|---------------------|-------------------------------------|
| Accession For       |                                     |
| NTIS GML&I          | <input checked="" type="checkbox"/> |
| IDC TAB             | <input type="checkbox"/>            |
| Unannounced         | <input type="checkbox"/>            |
| Justification       |                                     |
| By _____            |                                     |
| Distribution/ _____ |                                     |
| Availability Codes  |                                     |
| Dist                | Availand/or special                 |
| A                   |                                     |

## TABLE OF CONTENTS

|  | <u>Page</u> |
|--|-------------|
| 1.0 Introduction                             | 1           |
| 2.0 Experimental                             | 2           |
| 2.1 Temperature and Pressure                 | 2           |
| 2.2 Water/Solids Ratio and Relative Humidity | 3           |
| 2.3 X-Ray Diffraction                        | 3           |
| 2.4 Mass Spectroscopy                        | 3           |
| 2.5 Thermal Analysis                         | 3           |
| 2.6 Surface Area Measurements                | 4           |
| 2.7 Scanning Electron Microscopy             | 4           |
| 3.0 Results and Discussion                   | 4           |
| 3.1 Kinetics                                 | 4           |
| 3.2 Reaction Products                        | 10          |
| 3.3 Carbonation Reaction                     | 19          |
| 3.4 Strength                                 | 19          |
| 4.0 Summary                                  | 22          |
| 5.0 References                               | 26          |
| 6.0 Appendix 1                               | 27          |
| 7.0 Participating Scientific Personnel       | 32          |
| 8.0 Publications                             | 32          |

## LIST OF FIGURES

| <u>Figure</u> |   | <u>Page</u> |
|---------------|---|-------------|
| 1             | Relationship between C/S ratio of anhydrous calcium silicate and activated energy for the CO <sub>2</sub> -H <sub>2</sub> O-calcium silicate reaction.  | 5           |
| 2             | Plot of weight gain of $\gamma$ -C <sub>2</sub> S dry powder (w/s = 0) after prescribed reaction times in 100% C at various relative humidities.  | 7           |
| 3             | Degree of carbonation for anhydrous $\beta$ -C <sub>2</sub> S powder (3850 cm <sup>2</sup> /g)  | 8           |
| 4             | Degree of carbonation for anhydrous $\beta$ -C <sub>2</sub> S powder (5300 and 6300 cm <sup>2</sup> /g)   | 8           |
| 5             | Effect of w/s ratio on the degree of carbonation for $\beta$ -C <sub>2</sub> S and C <sub>3</sub> S powders   | 9           |
| 6             | Degree of reaction as a function of time of dry $\beta$ -CS powder reacted at 23°C, 100% RH, 100% C at various C pressures.   | 11          |
| 7             | Degree of reaction as a function of time of moist $\gamma$ -CS powder reacted at 23°C, 100% RH, 100% C at various C pressures   | 11          |
| 8             | Degree of carbonation across the diameter of calcium silicate pellets   | 12          |
| 9             | Photomicrograph of 92% reacted $\gamma$ -C <sub>2</sub> S powder which was initially moistened (w/s 0.15) and carbonated in a 1 atmosphere CO <sub>2</sub> , 100% relative humidity, 23°C environment for 10,935 minutes (7.6 days). Figure 9B is an enlargement of 9A. The granular surface material is the CaCO <sub>3</sub> reaction product which consists of a mixture of calcite and aragonite.   | 14          |
| 10            | Photomicrograph of 97% reacted $\gamma$ -C <sub>2</sub> S powder which was initially moistened (w/s 0.15) and carbonated in a 54 atmosphere CO <sub>2</sub> , 100% relative humidity, 23°C environment for 10,935 minutes (7.6 days). Figure 10B is an enlargement of 10A. The granular surface material is the CaCO <sub>3</sub> reaction product which consists of a mixture of calcite and aragonite. The individual granules are about twice the size of those shown in Figure 9. | 15          |
| 11            | Photomicrograph of 55% reacted $\beta$ -CS powder which was initially dry and carbonated in 54 atmospheres, 100% relative humidity, 23°C environment for 10,935 minutes (7.6 days). Figure 11B is an enlargement of 11A. The lath shaped CaCO <sub>3</sub> reaction product is aragonite.   | 16          |

| <u>Figure</u> |  | <u>Page</u> |
|---------------|--|-------------|
| 12            | The C/S ratio of the C-S-H reaction product of carbonated $\beta$ -CS as a function of degree of reaction.   | 17          |
| 13            | Amount of carbonate formation versus degree of carbonation of $\beta$ -C <sub>2</sub> S powders of different w/s ratios. The theoretical carbonate/cement ratio line represents a C-S-H reaction product with C/S = 0. The greater the divergence from the theoretical carbonate/cement ratio line the higher the C/S in the C-S-H reaction product. | 18          |
| 14            | Interrelationship between water specific surface area and C/S ratio of C-S-H produced during the carbonation of $\gamma$ -C <sub>2</sub> S   | 20          |
| 15            | Interrelationship between water specific surface area and H/S ratio of C-S-H produced during the carbonation of $\gamma$ -C <sub>2</sub> S   | 21          |
| 16            | Relationship of compressive strength to capillary porosity of carbonated and hydrated compacted materials.   | 23          |

## 1.0 Introduction

Investigations into the carbonation of hydraulic and non-hydraulic calcium compounds such as portland cement, lime, and calcium silicates have accelerated in the past few years. References dealing with the carbonation hardening of various hydraulic and non-hydraulic calcium binders increased from 1 in 1974 to 29 in 1978, as reported in Cements Research Progress<sup>1,2</sup>. The references reported in 1978 included 17 Japanese patents based on the carbonation of various binders and glass fiber-reinforced systems. The potential for carbonated cement systems is great since low energy calcium compounds can be reacted with a waste resource, CO<sub>2</sub>, to produce high strength durable building units. However, basic studies of the carbonation reactions are few and the present investigation is designed to provide information on the reaction kinetics, reaction products and the reaction mechanism of the carbonation process. In the present work the reaction of five calcium silicates, Ca<sub>3</sub>SiO<sub>5</sub> (C<sub>3</sub>S)\*, β-Ca<sub>2</sub>SiO<sub>4</sub> (β-C<sub>2</sub>S), γ-Ca<sub>2</sub>SiO<sub>4</sub> (γ-C<sub>2</sub>S), Ca<sub>3</sub>SiO<sub>7</sub> (C<sub>3</sub>S<sub>2</sub>) and β-CaSiO<sub>3</sub> (β-CS) were studied. In all cases the reaction of CO<sub>2</sub> (C̄) and H<sub>2</sub>O (H) with calcium silicates resulted in the formation of reaction products consisting of CaCO<sub>3</sub> (C̄C) and a low lime calcium silicate hydrate (C-S-H).

Excellent reviews of the carbonation of calcium silicate containing materials are presented elsewhere.<sup>3,4</sup>

---

\*Cement chemist's shorthand nomenclature is hereafter employed: C = CaO, S = SiO<sub>2</sub>, H = H<sub>2</sub>O, C̄ = CO<sub>2</sub>.

## 2.0 Experimental

The effect of temperature,  $\text{CO}_2$  pressure, partial pressure of  $\text{CO}_2$ , water/solids ratio (w/s), relative humidity (RH), and fineness on the carbonation reaction of various calcium silicates was studied. The  $\beta$ -CS, a naturally occurring mineral, was obtained from Cabot Corp.\*, while the  $\text{C}_3\text{S}_2$ ,  $\gamma$ - $\text{C}_2\text{S}$ ,  $\beta$ - $\text{C}_2\text{S}$  (stabilize with magnesium and aluminum) and  $\text{C}_3\text{S}$  were prepared from reagent grade chemicals. All the calcium silicates were ground to a Blaine fineness of approximately  $5000 \text{ cm}^2/\text{g}$ ; in addition, the  $\beta$ - $\text{C}_2\text{S}$  and  $\text{C}_3\text{S}$  were ground to approximately 4000 and  $6000 \text{ cm}^2/\text{g}$  to test the influence of fineness on reaction rate. All calcium silicates were reacted in 100% RH, 100%  $\text{CO}_2$  environmental chambers. A schematic of the reaction chambers used in the  $\beta$ - $\text{C}_2\text{S}$ ,  $\text{C}_3\text{S}$ ,  $\beta$ -CS and  $\text{C}_3\text{S}_2$  studies are shown in Figure 1, Appendix 1. The  $\beta$ -CS and  $\gamma$ - $\text{C}_2\text{S}$  were reacted in a similar manner in a high pressure bomb\*\* rather than dessicators. The experimental procedures such as sample preparation and carbonation as well as the analytical techniques including qualitative and quantitative x-ray diffraction analysis (QXDA), specific gravity,  $\text{H}_2\text{O}$  surface area measurements, thermogravimetric analysis (TGA), mass spectrometry, stepwise constant temperature pyrolysis, and scanning electron microscopy (SEM) for  $\beta$ - $\text{C}_2\text{S}$  and  $\text{C}_3\text{S}$  and  $\beta$ -CS and  $\gamma$ - $\text{C}_2\text{S}$  are discussed in detail by Goodbrake<sup>3</sup> and Ghinazzi<sup>4</sup>, respectively.

### 2.1 Temperature and Pressure

Samples of  $\text{C}_3\text{S}$ ,  $\beta$ - $\text{C}_2\text{S}$  and  $\beta$ -CS were reacted at  $5^\circ$ ,  $25^\circ$ ,  $40^\circ$  and  $60^\circ\text{C}$ . In another set of experiments,  $\text{C}_3\text{S}$  and  $\beta$ - $\text{C}_2\text{S}$  were reacted at partial pressures of  $\text{CO}_2$  from 0.025 to 1.0. Gamma- $\text{C}_2\text{S}$  and  $\beta$ -CS were reacted at  $\text{CO}_2$  pressures of 1, 4, and 54 atm.

---

\* Cabot Corporation, Boston, Mass.

\*\* Parr Instrument Co., Moline, IL.

## 2.2 Water/Solids Ratio and Relative Humidity

The initial water/solids ratio was varied from 0.0 to 0.3. The water vapor saturation of the CO<sub>2</sub> reaction chamber was 100% in the majority of tests. However, in order to determine the influence relative humidity plays on the carbonation reaction, a series of tests were performed in which the water vapor saturation of the CO<sub>2</sub> in the reaction chamber was varied from 10 to 100%.

## 2.3 X-Ray Diffraction

Qualitative x-ray diffraction was used to determine the polymorphic type of calcium carbonate which formed during the reaction of calcium silicates with CO<sub>2</sub> and water. Quantitative x-ray diffraction was used to determine the degree of reaction by measuring the amount of residual calcium silicate after given reaction periods and in some cases the quantity of the calcium carbonate reaction products, aragonite and calcite. These data were used in determining the reaction kinetics as well as the stoichiometry of the calcium silicate hydrate (C-S-H) reaction product.

## 2.4 Mass Spectrometry

Mass spectrometry was used to determine the nature of the decomposition products during a programmed heating of reacted samples. It was found that only H was present in the volatile decomposition products up to 400°C, and only  $\bar{C}$  was present at temperatures >400°C.

## 2.5 Thermal Analysis

Thermogravimetric and stepwise constant temperature pyrolysis were used to determine the H contents and  $\bar{C}$  contents of reacted samples. The  $\bar{C}$  content was used to determine the quantity of  $C\bar{C}$  present in the reaction

product. The stoichiometry of the C-S-H reaction product was determined indirectly from the  $\text{C}\bar{\text{C}}$  and H contents determined by thermal analysis and the degree of reaction determined by quantitative x-ray diffraction analysis.

## 2.6 Surface Area Measurements

Both nitrogen and water vapor surface areas were determined to provide some insight into the nature of the reaction products.

## 2.7 Scanning Electron Microscopy

Scanning electron microscopy was used to determine the morphological nature of the reaction products which included two polymorphs of  $\text{C}\bar{\text{C}}$ , aragonite and calcite, as well as C-S-H.

## 3.0 Results and Discussion

### 3.1 Kinetics

The reaction kinetics were determined on dry calcium silicate powders (i.e., the initial calcium silicate having a w/s ratio of 0) because the reactions in these tests were reproducible and not influenced by secondary parameters. Calcium silicates with w/s > 0 react very rapidly initially and self-desiccate resulting in a significant slow down in the reaction. This system was difficult to maintain under controlled conditions which resulted in a reaction which was difficult to reproduce and interpret. A detailed discussion of the reaction kinetics of  $\text{C}_3\text{S}$  and  $\beta\text{-C}_2\text{S}$  reactions are given in Appendix 1. The reaction of all calcium silicates followed the same general diminishing volume diffusion controlled kinetic model. The kinetics of the reaction are controlled by the C/S ratio of the starting calcium silicate. A plot of the C/S ratio versus activation energy is shown in Figure 1.

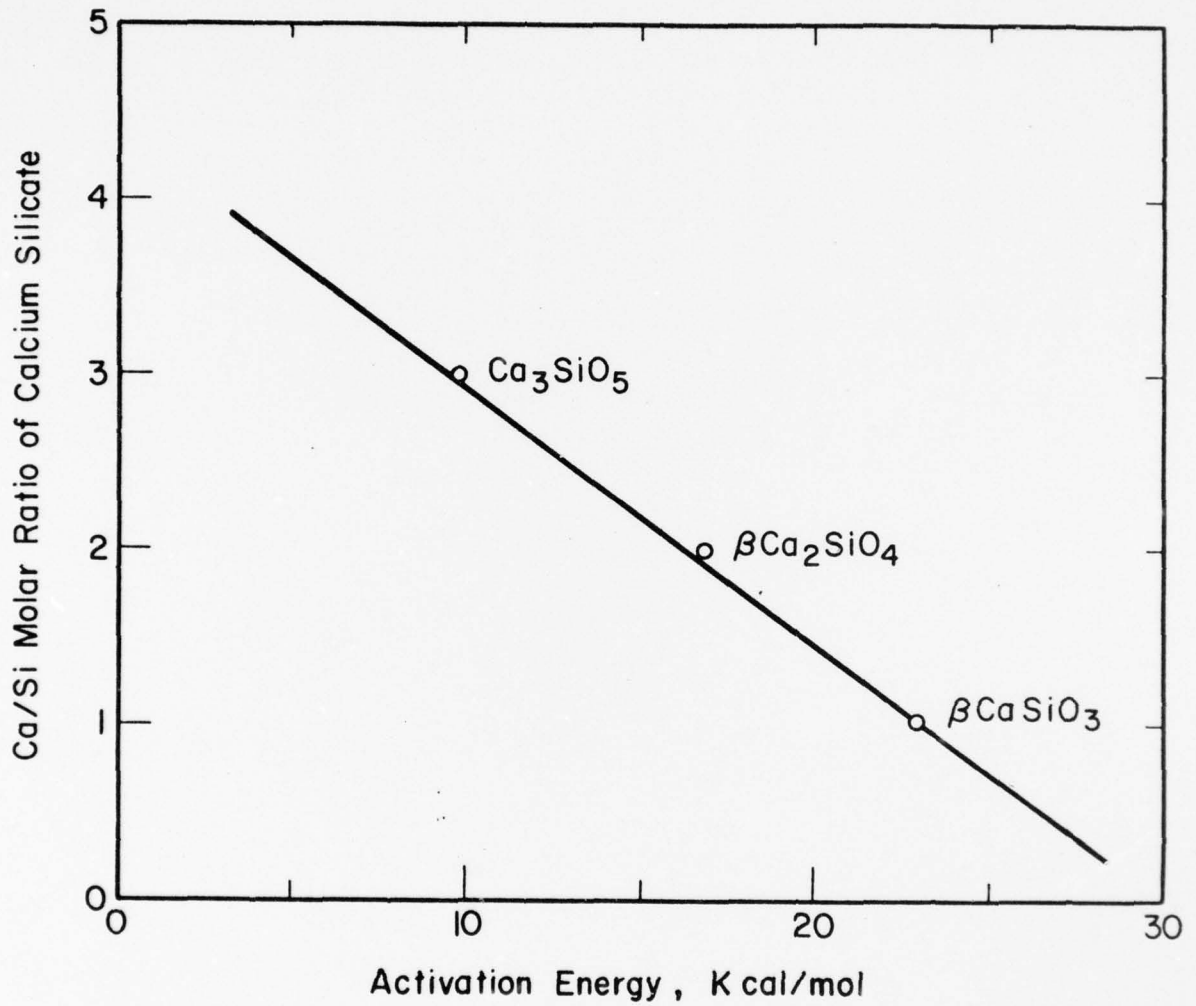


Figure 1. Relationship between C/S ratio of anhydrous calcium silicate and activation energy for the  $\text{CO}_2\text{-H}_2\text{O}$ -calcium silicate reaction.

The influence of partial pressure of  $\bar{C}$  on the reaction kinetics are shown in Figure 4A, Appendix 1. The rapid carbonation reaction experienced at partial pressures above 0.12 atm diminish below 0.12 atm and very little carbonation occurs below 0.025 atm during the time period studied. The influence of RH on the reaction kinetics is shown in Figure 4B of Appendix 1 for  $C_3S$  and  $\beta-C_2S$ . Over a 24 hour reaction time there is a steady decline in reactivity with declining RH from 100 to 0%. However, for  $\gamma-C_2S$  the RH has a very strong influence on degree of reaction as indicated by the plot of weight gain/g  $C_2S$  versus RH shown in Figure 2. For long-term carbonations the degree of reaction falls off very rapidly at RH values below 100% and the reaction ceases in all cases at  $RH < 40\%$ .

The strong dependency of the  $\beta-C_2S$  reaction rate on temperature is shown in Figures 3 and 4. The influence of fineness on reaction rate is also shown in Figure 4. Temperature is the predominate influence on the rate of reaction with all the calcium silicates studied.

The influence of w/s ratio on degree of reaction after a 24 hour reaction period in a 100%  $\bar{C}$  and 100% RH environment is shown in Figure 5 for  $C_3S$  and  $\beta-C_2S$ . Maximum reactivity takes place at a 0.10 w/s ratio for  $\beta-C_2S$  and approximately 0.15 for  $C_3S$ . The decrease in reactivity with increasing w/s ratio is a result of pores between particles being filled with water and blocking the ingress of  $CO_2$  to the powder surfaces. At w/s below the optimum, reactivity decreases due to the lack of water at the interface. This water must be obtained from the atmosphere and diffuse into the sample, thus resulting in a slower reactivity. The optimum w/s ratios change with the length of reaction time. With an increased reaction time, the optimum w/s moves to lower values. The influence of increasing the

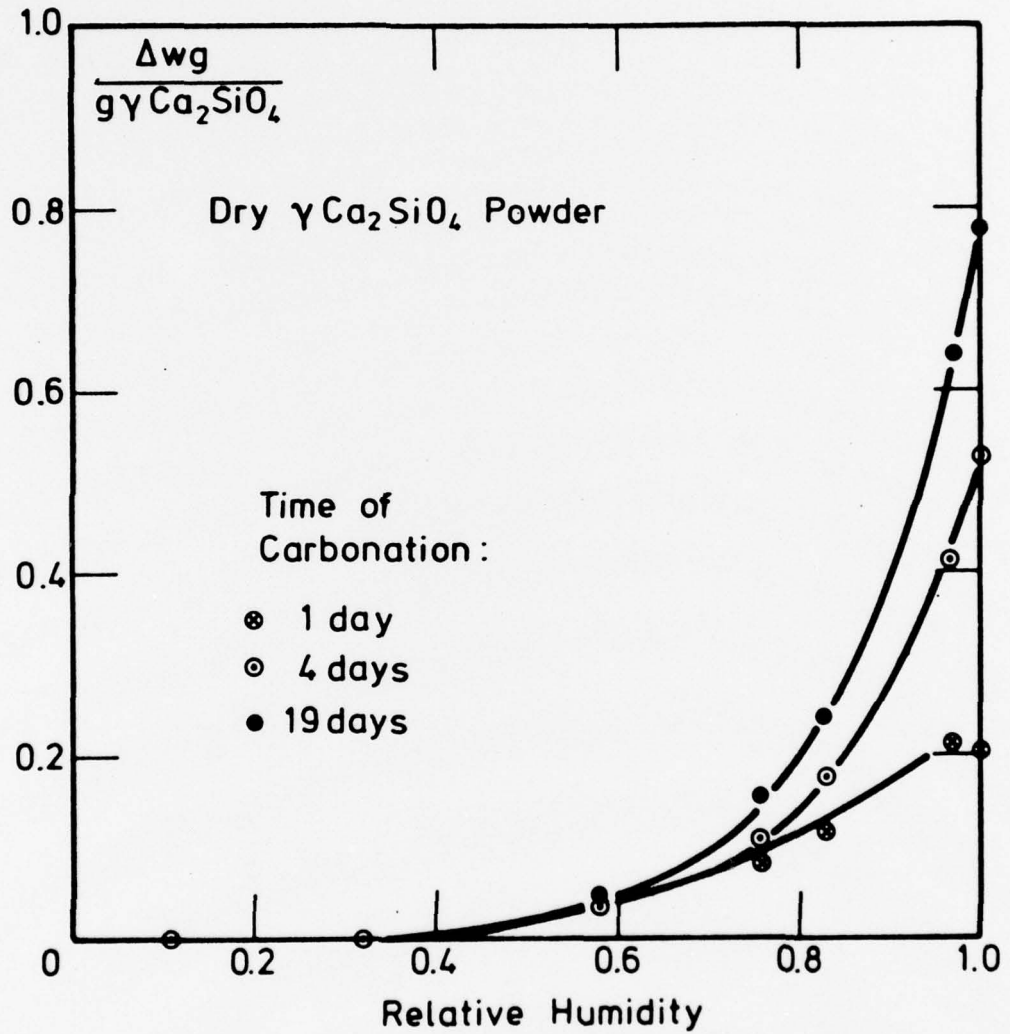


Figure 2. Plot of weight gain of  $\gamma\text{-C}_2\text{S}$  dry powder ( $w/s = 0$ ) after prescribed reaction times in 100% C at various relative humidities.

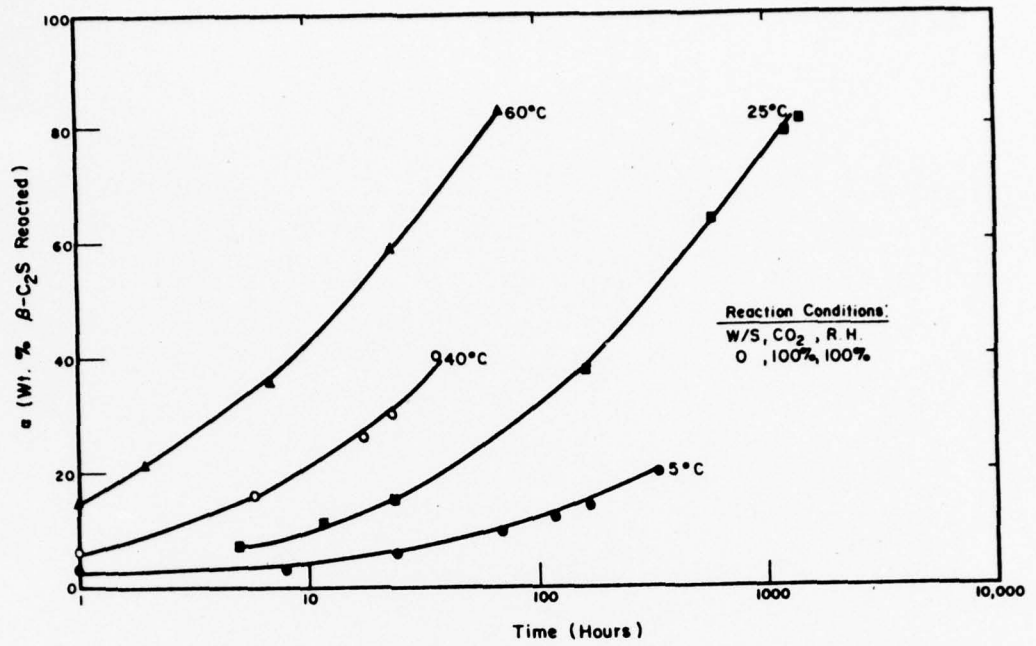


Figure 3. Degree of carbonation for anhydrous  $\beta$ -C<sub>2</sub>S powder (3850 cm<sup>2</sup>/g)

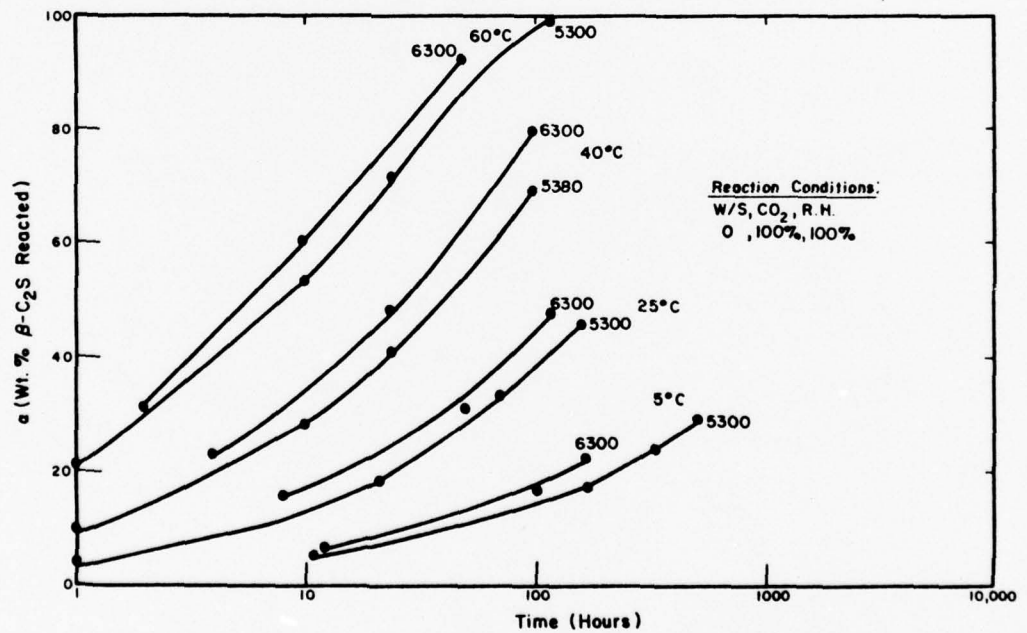


Figure 4. Degree of carbonation for anhydrous  $\beta$ -C<sub>2</sub>S powder (5300 and 6300 cm<sup>2</sup>/g)

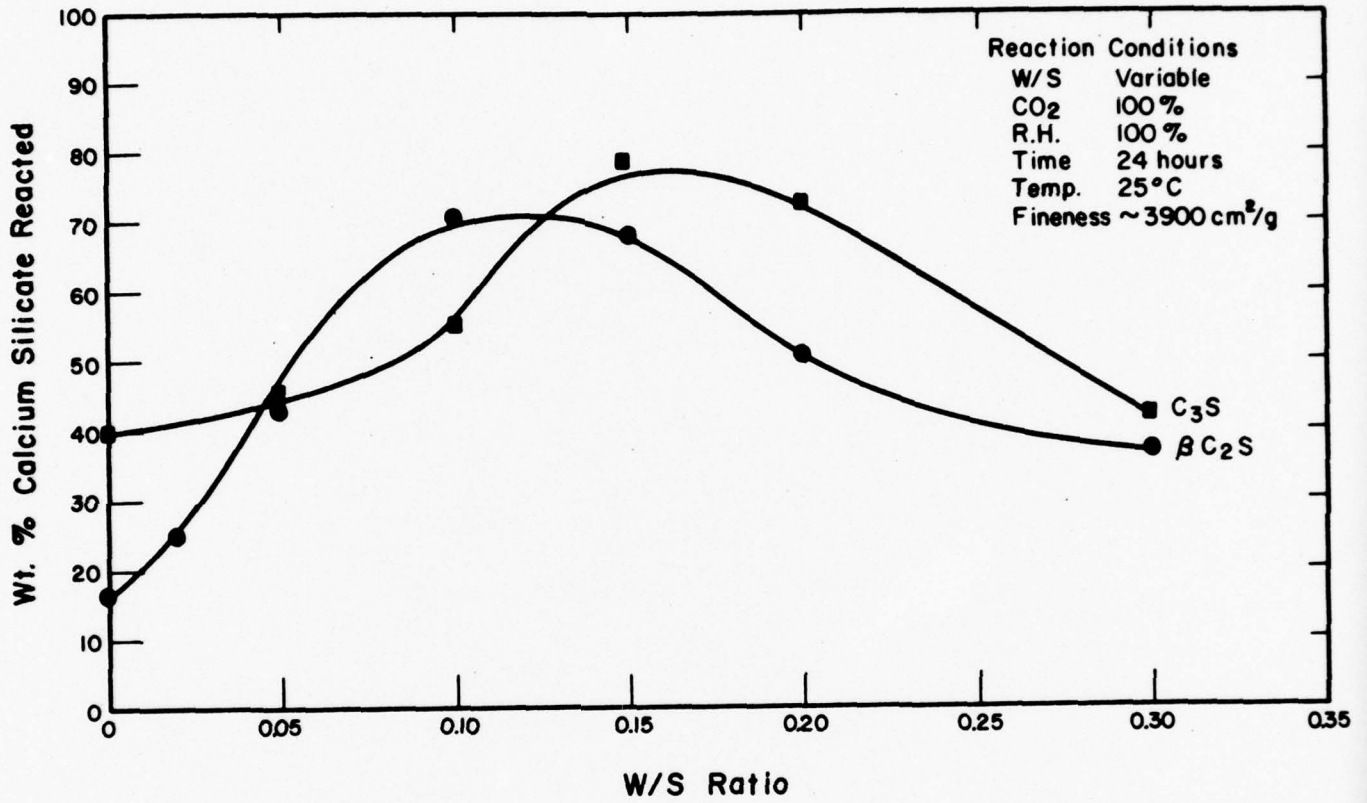


Figure 5. Effect of w/s ratio on the degree of carbonation for  $\beta$ -C<sub>2</sub>S and C<sub>3</sub>S Powders

$\bar{C}$  pressure from 1 to 54 atm on the reactivity of  $\beta$ -CS and  $\gamma$ -C<sub>2</sub>S were studied in 100% RH environments and with w/s ratios of 0 and 0.15. The effect of increasing the  $\bar{C}$  pressure was difficult to interpret since the test results were difficult to reproduce; but in general, increasing the pressure did result in some increase in the degree of reaction. The degrees of reaction versus reaction time of dry and wet (w/s 0.15)  $\beta$ -CS powders reacted at 1, 4 and 54 atm of  $\bar{C}$  are shown in Figures 6 and 7. In all cases the influence of  $\bar{C}$  pressure on reactivity was not as great as moderate increases in temperature.

The diffusion of  $\bar{C}$  into wet and dry compacted samples of  $\beta$ -C<sub>2</sub>S, C<sub>3</sub>S, and a mixture of  $\beta$ -C<sub>2</sub>S and C<sub>3</sub>S, was investigated by determining the degree of carbonation through a cross-section of the compact after various times of carbonation. In all cases the degree of reaction was highest in the 1 mm surface layer. In the dry samples the reaction was equal throughout the remainder of the compacts with the degree of carbonation increasing with time of reaction. In the wet compacts the reaction was faster and the degree of reaction diminished continuously towards the center of the compact with the exception after long term reaction times where the reaction became fairly even throughout the cross section of the compact (Fig. 8).

### 3.2 Reaction Products

The reaction products of the carbonation reaction with all the calcium silicates studied were C $\bar{C}$  and a C-S-H with variable stoichiometry. Two C $\bar{C}$  polymorphs were predominant. Calcite generally occurred in samples which contained H whereas aragonite formed during the carbonation of the initially dry calcium silicates (w/s = 0), during the later stages of reaction in the other calcium silicate systems with w/s > 0 and in wet  $\beta$ -CS. The C $\bar{C}$  formed outside the original calcium silicates grain boundaries and was the

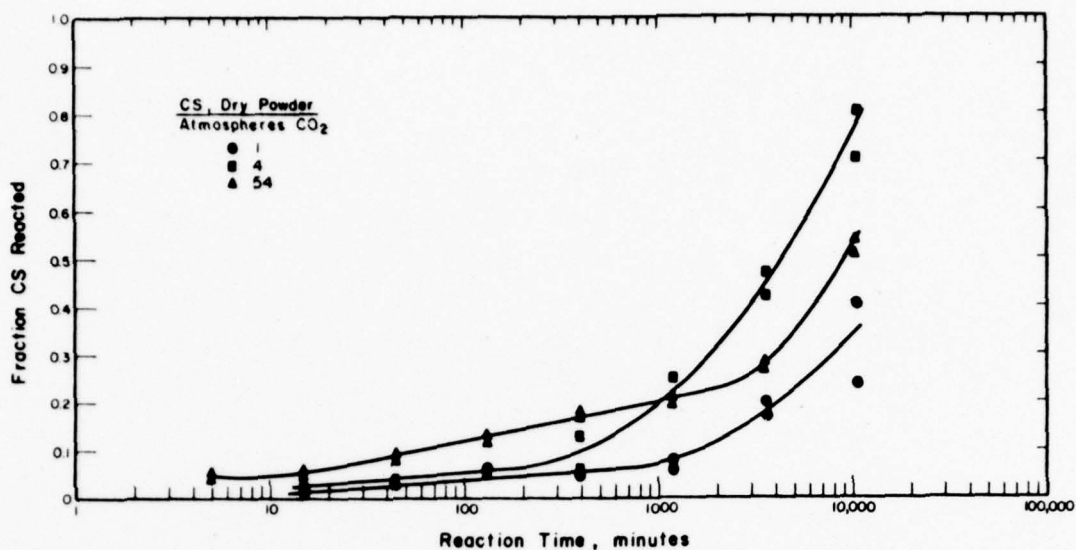


Figure 6. Degree of reaction as a function of time of dry  $\beta$ -CS powder reacted at 23°C, 100% RH, 100%  $\bar{C}$  at various  $\bar{C}$  pressures.

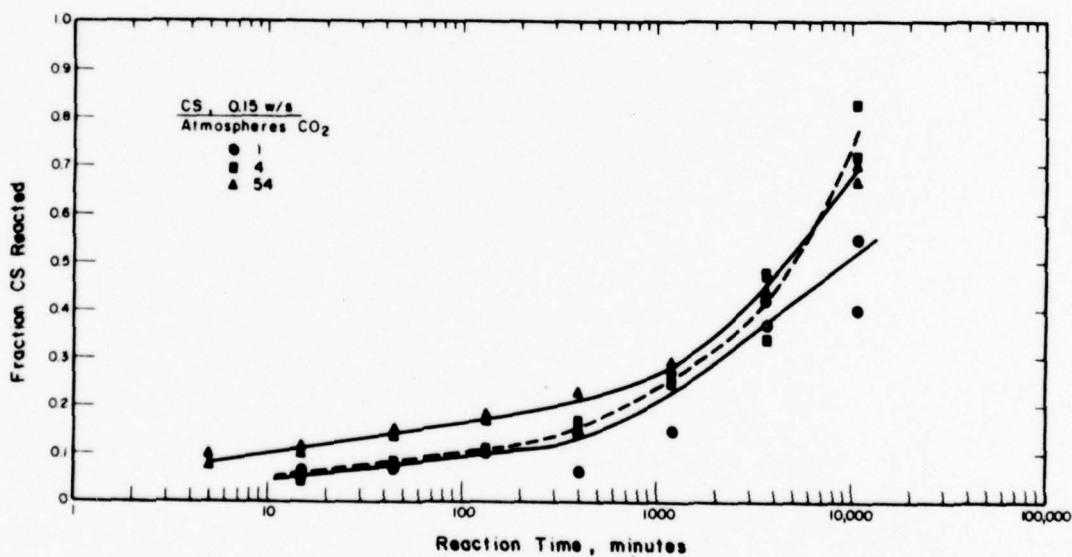


Figure 7. Degree of reaction as a function of time of moist  $\gamma$ -CS powder reacted at 23°C, 100% RH, 100%  $\bar{C}$  at various  $\bar{C}$  pressures.

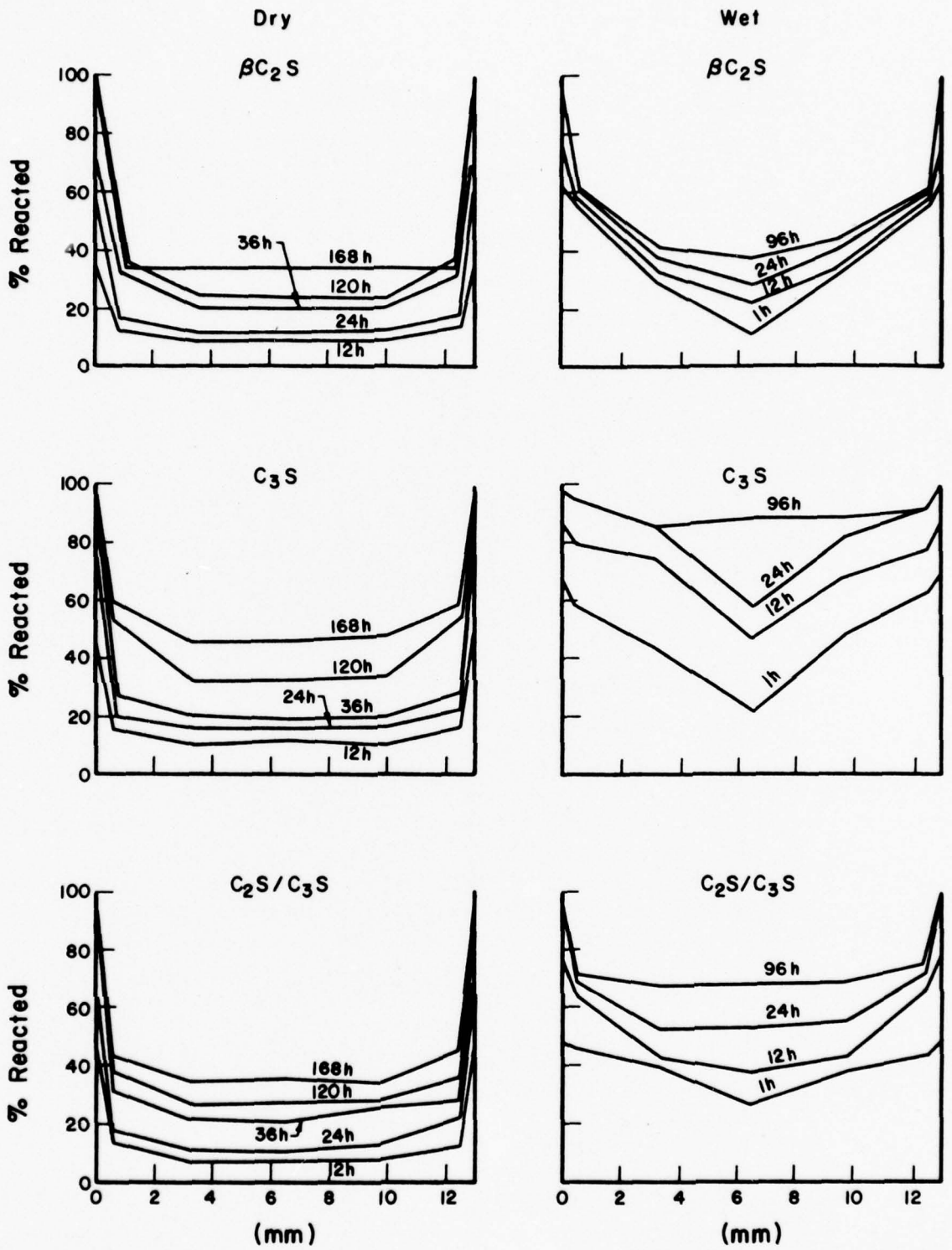


Figure 8. Degree of carbonation across the diameter of calcium silicate pellets

only reaction product observed with SEM (Figure 7, Appendix 1; Fig. 9). In the carbonation of  $\gamma\text{-C}_2\text{S}$  an increase in  $\bar{C}$  pressure resulted in larger  $\bar{C}\bar{C}$  crystals (Fig. 9 and 10). Aragonite which formed during the carbonation of  $\beta\text{-CS}$  is shown in Fig. 11. Numerous SEM photos of the  $\bar{C}\bar{C}$  reaction products of  $\beta\text{-CS}$  and  $\gamma\text{-C}_2\text{S}$ , and  $\beta\text{-C}_2\text{S}$  and  $\text{C}_3\text{S}$  are presented by Ghinazzi<sup>4</sup> and Goodbrake<sup>3</sup>, respectively.

The C-S-H reaction product forms primarily within the grain boundary of the original anhydrous powder. This reaction product in carbonated  $\text{C}_3\text{S}$  and  $\beta\text{-C}_2\text{S}$  initially has a high C/S and H/S ratio which decreases as the carbonation continues (Figure 6, Appendix 1). The C/S ratio in the C-S-H formed during the carbonation of  $\gamma\text{-C}_2\text{S}$  and  $\beta\text{-CS}$  is initially low and increases to a maximum and then decreases as shown in Fig. 12 for  $\beta\text{-CS}$ . The H/S ratio for all other systems studied decrease with increasing reactivity, similar to that shown for  $\beta\text{-C}_2\text{S}$  and  $\text{C}_3\text{S}$  (Figure 6B, Appendix 1). An increase in the initial w/s results in a general increase in the C/S ratio of the C-S-H. This is shown indirectly in Fig. 13 where the larger the deviation from the theoretical carbonate/cement ratio line represents a higher C/S ratio of the C-S-H. The resulting C-S-H after high degrees of reaction is almost a hydrous amorphous silica as the  $\bar{C}$  reacts with the C-S-H to remove C. The C-S-H reaction product is insoluble in hydrochloric acid. The C-S-H product after dissolution in acid has the same morphology as the original starting anhydrous calcium silicate, indicating that C has been pulled out of the anhydrous calcium silicates to form  $\bar{C}\bar{C}$  leaving the S behind which forms a highly polymerized insoluble structure.

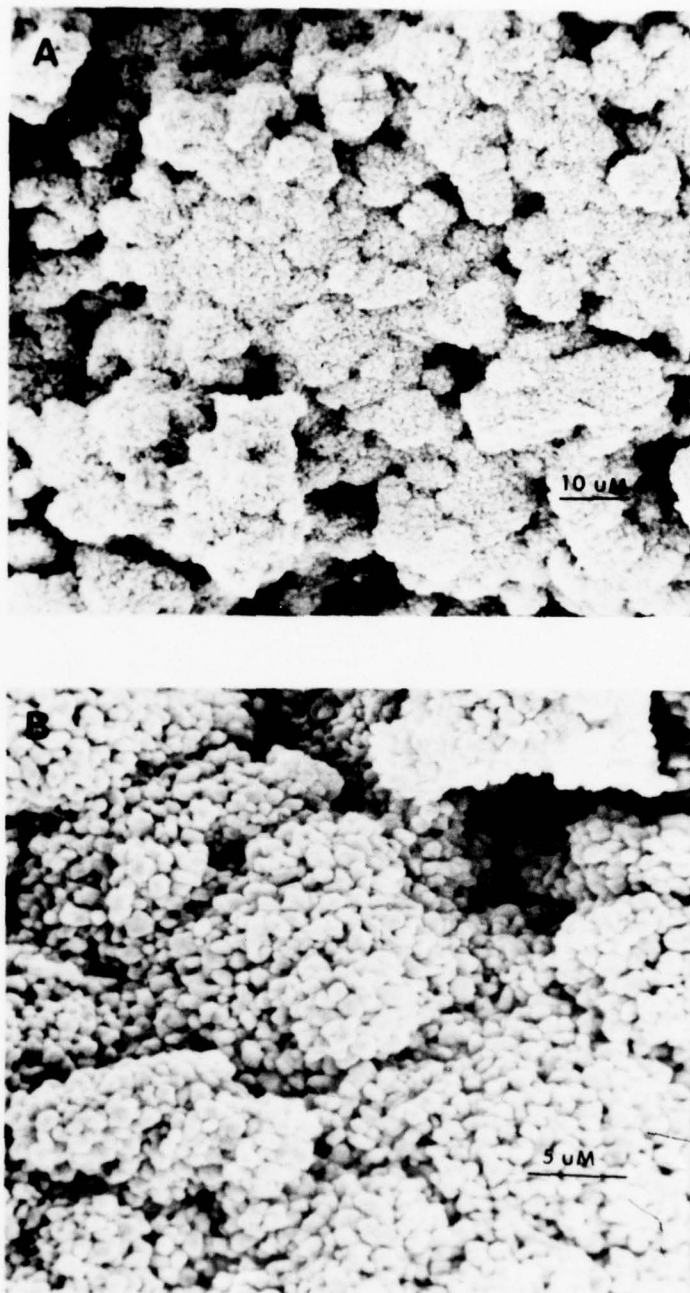


Figure 10. Photomicrograph of 97% reacted  $\gamma$ -C<sub>2</sub>S powder which was initially moistened (w/s 0.15) and carbonated in a 54 atmosphere CO<sub>2</sub>, 100% relative humidity, 23°C environment for 10,935 minutes (7.6 days). Figure 10B is an enlargement of 10A. The granular surface material is the CaCO<sub>3</sub> reaction product which consists of a mixture of calcite and aragonite. The individual granules are about twice the size of those shown in Figure 9.

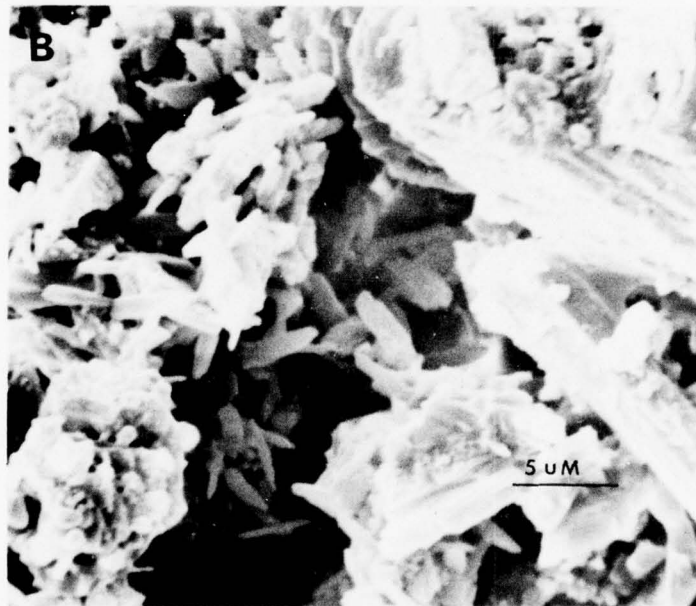
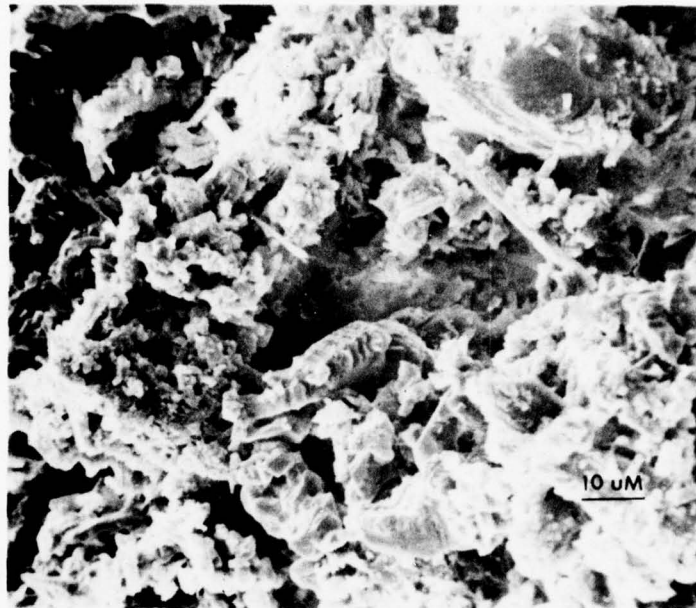


Figure 11. Photomicrograph of 55% reacted  $\beta$ -CS powder which was initially dry and carbonated in 54 atmospheres, 100% relative humidity, 23°C environment for 10,935 minutes (7.6 days). Figure 11B is an enlargement of 11A. The lath shaped  $\text{CaCO}_3$  reaction product is aragonite.

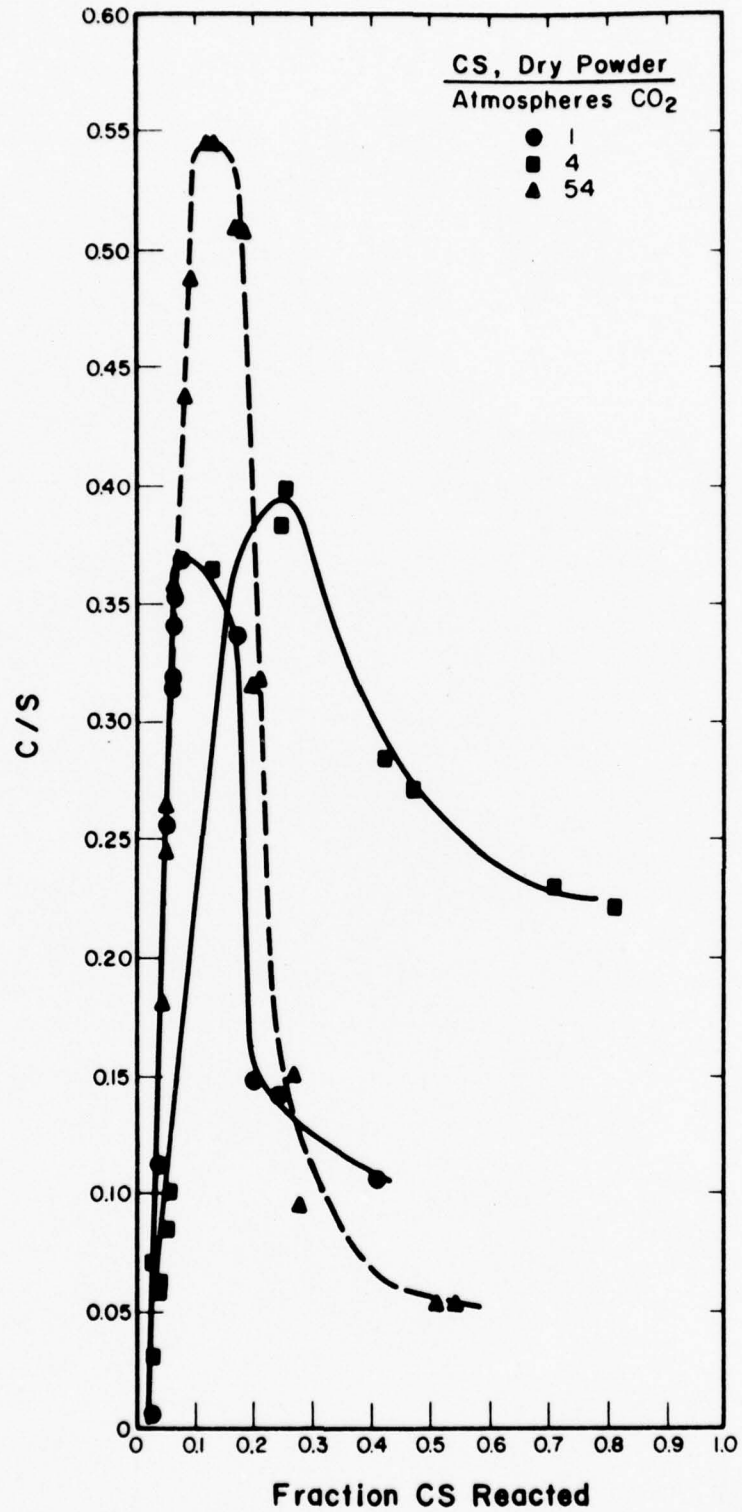


Figure 12. The C/S ratio of the C-S-H reaction product of carbonated  $\beta$ -CS as a function of degree of reaction.

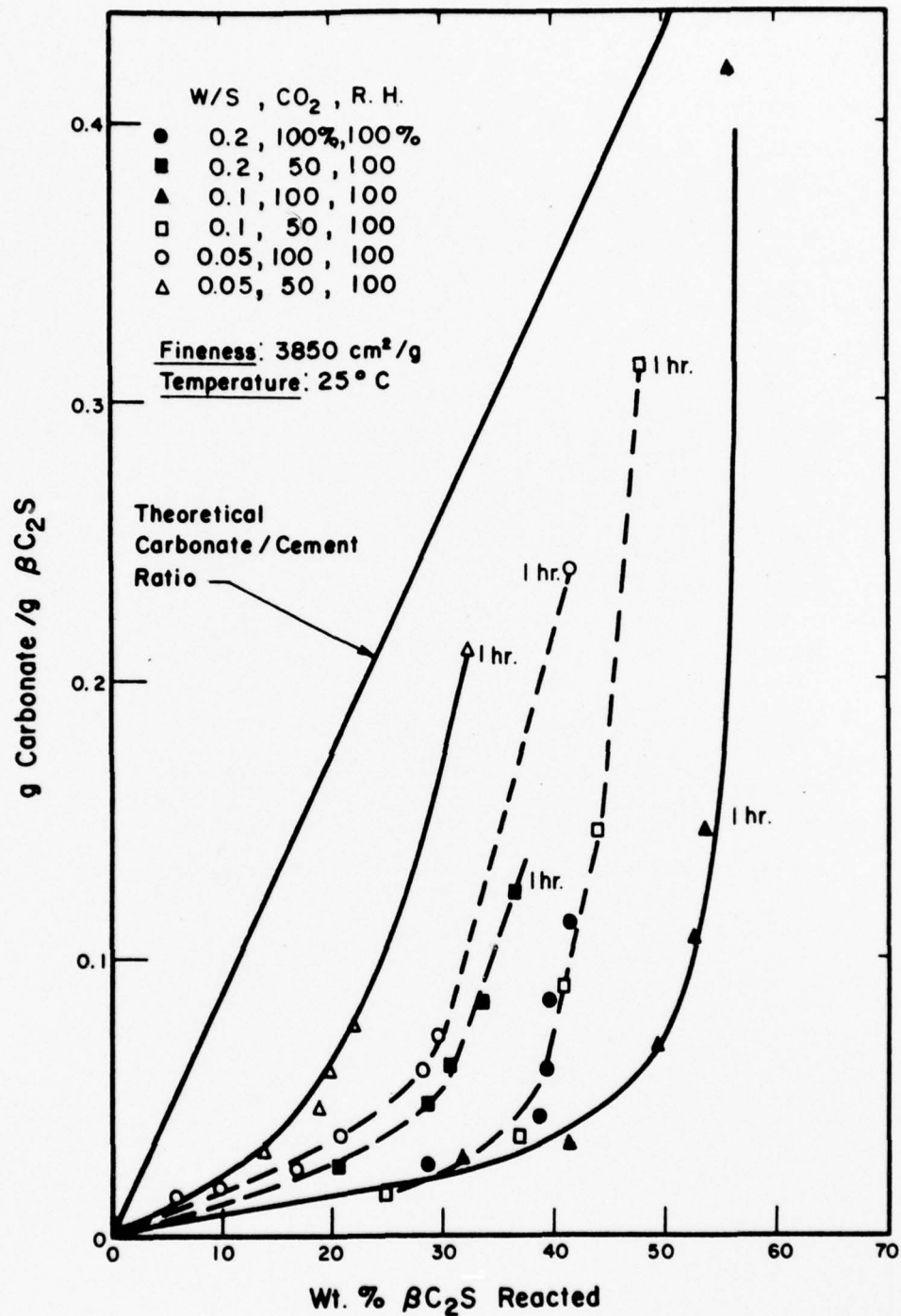
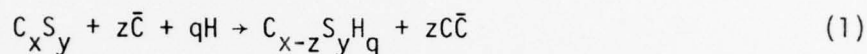


Figure 13. Amount of carbonate formation versus degree of carbonation of  $\beta$ -C<sub>2</sub>S powders of different w/s ratios. The theoretical carbonate/cement ratio line represents a C-S-H reaction product with C/S = 0. The greater the divergence from the theoretical carbonate/cement ratio line the higher the C/S in the C-S-H reaction product.

The H surface area of the C-S-H in carbonated  $C_3S$ ,  $\beta$ - $C_2S$  and  $\gamma$ - $C_2S$  decreases from 300-400  $m^2/g$  to approximately 100  $m^2/g$ , as the reaction continues from 20 to 80%<sup>3,5</sup>. However, some work<sup>4</sup> has shown that the surface area of carbonated  $\gamma$ - $C_2S$  increased with degree of reaction and also increased with a decrease in the C/S and H/S ratios of the C-S-H (Figs. 14 and 15).

### 3.3 Carbonation Reaction

From the proceeding data the general carbonation reactions for all the calcium silicates can be expressed by



where  $x = 1, 2$  or  $3$ ,  $y = 1$  or  $2$ ,  $z = 1$  to  $3$ , and  $q = 0.2$  to  $3$ .

However, the C-S-H is a metastable phase in the presence of  $\bar{C}$ . Therefore, as carbonation progresses  $\bar{C}$  will react with the C-S-H to form additional  $C\bar{C}$  and a stable silica gel (S-H). Thus the final overall reaction can be expressed by



where  $x = 1, 2$  or  $3$ ;  $y = 1$  or  $2$  and  $q = 0.1$  to  $0.3$ .

### 3.4 Strength

Compressive and in some cases tensile strengths were determined on samples of  $\gamma$ - $C_2S$ ,  $\beta$ - $C_2S$ , and  $C_3S$  which were compacted at 21 MPa (3 ksi) into 7.9 or 5.6 mm dia. cylinders and carbonated for various lengths of times. In a few cases strength tests were made on samples which were hydrated and then carbonated or carbonated then hydrated for various time intervals. The capillary porosities of the pellets were determined by vacuum saturation with water and subsequent drying to 105°C. The strength

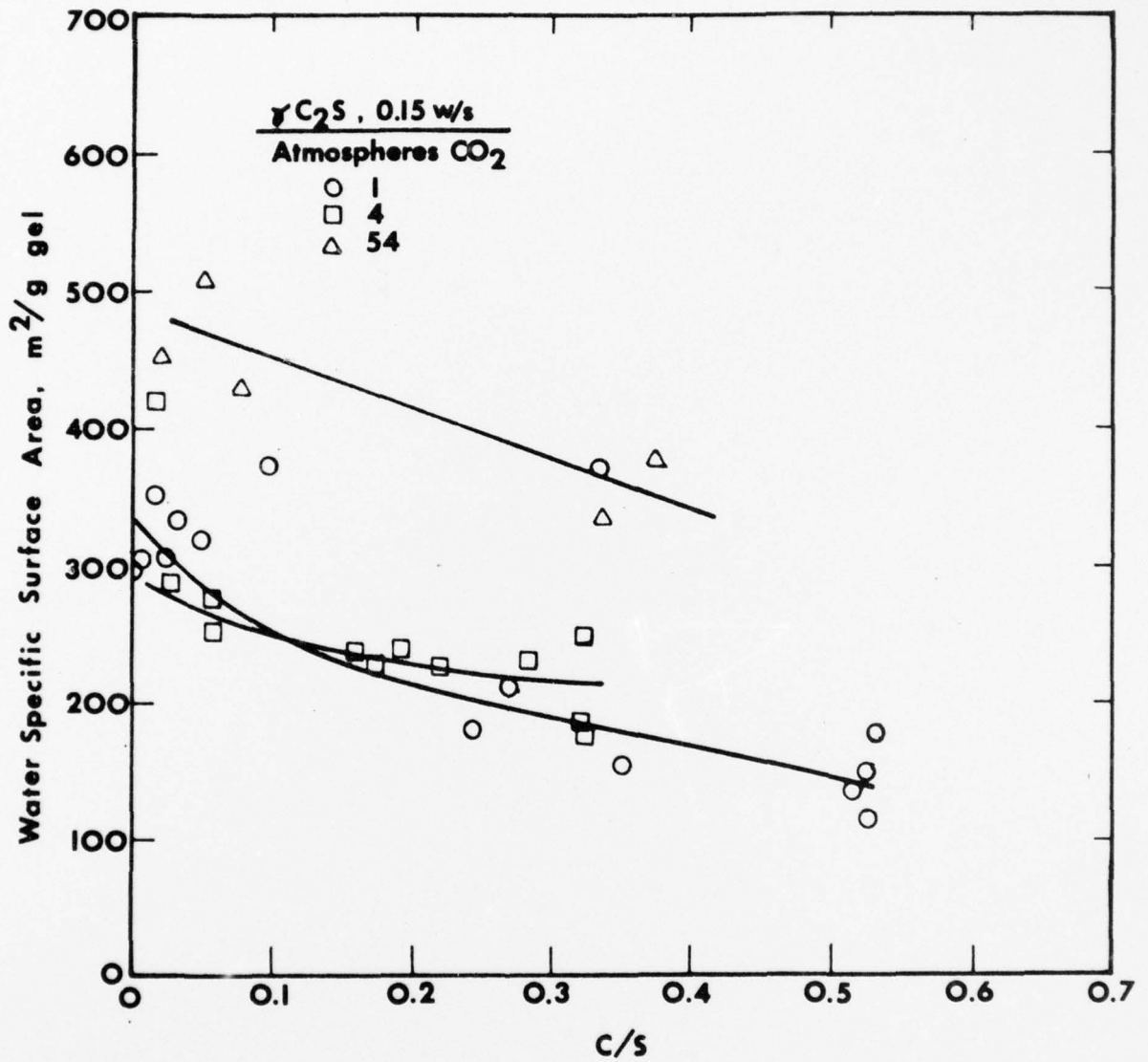


Figure 14. Interrelationship between water specific surface area and C/S ratio of C-S-H produced during the carbonation of  $\gamma$ -C<sub>2</sub>S.

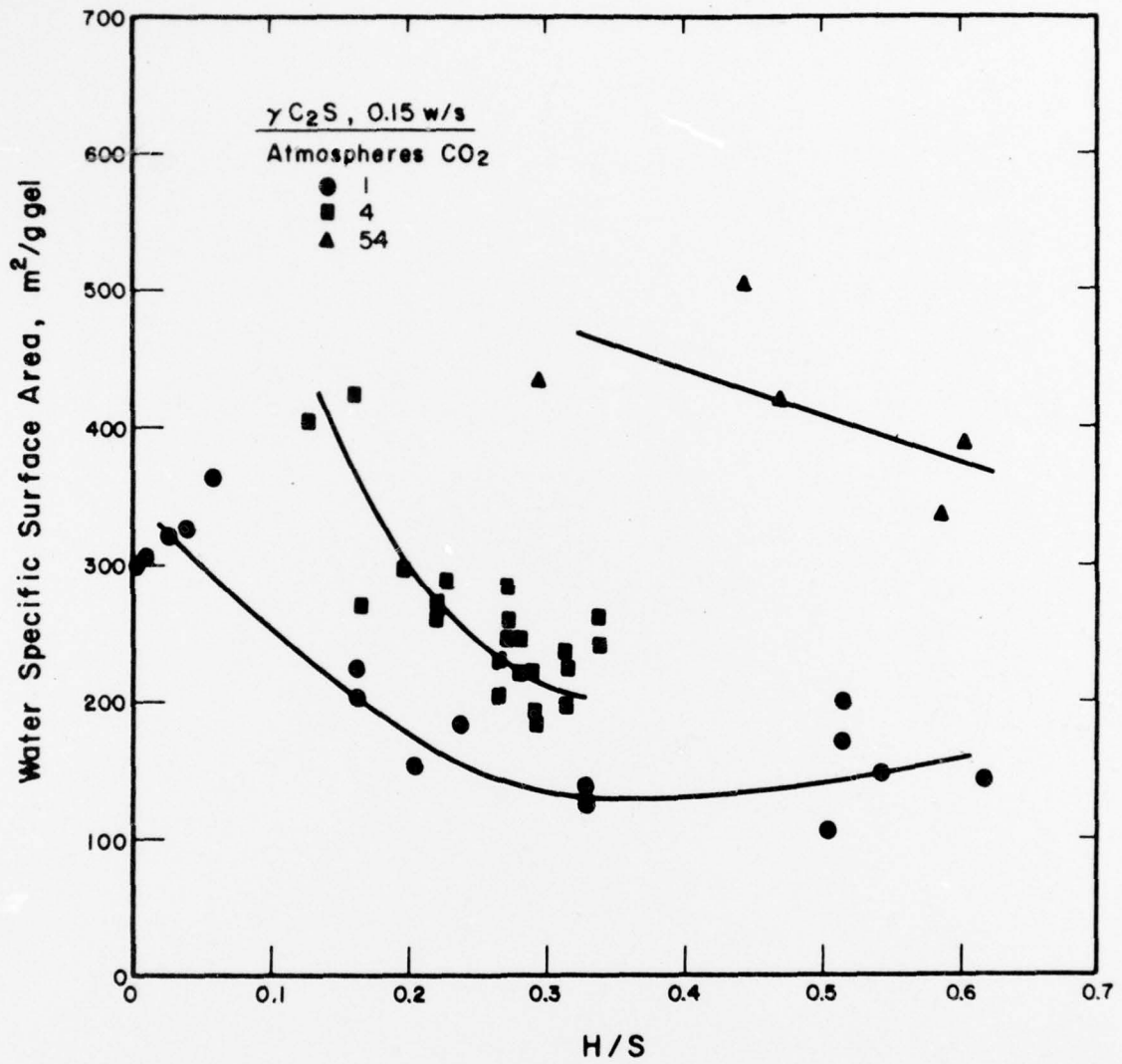


Figure 15. Interrelationship between water specific surface area and H/S ratio of C-S-H produced during the carbonation of  $\gamma\text{-C}_2\text{S}$ .

porosity relationship for some typical data is shown in Figure 16. This strength porosity relationship is similar to that developed by Roy and Gouda<sup>6</sup> for specimens compacted at high pressures (50-75 ksi) and hydrated. The fall off in strength development (Figure 16) under 30% (0.3) porosity, is due to the low degree of reactivity as the initial porosity of the unreacted compacts was ~40%. The advantage of the carbonated system is that a cementitious binder with a strength > 200 MPa develops upon carbonation in samples which were compacted at reasonably low initial compaction pressures. In hydrated cements compacted to the same initial porosity a strength development of only 150 MPa was possible. The intrinsic strength of the hydrated and carbonated systems seems to be approximately the same as the over-riding parameter in controlling strength is the capillary porosity.

#### 4.0 Summary

The objectives of the present study were to learn more about the reaction of calcium silicates with  $\text{CO}_2$  and water. The properties of the carbonation products, kinetics of the carbonation reaction, and mechanism of carbonation were studied within the scope of the present investigation. The carbonation of five calcium silicate systems which differed in composition or polymorphism were considered. Specific findings included:

- 1) Reaction kinetics depend on the Ca/Si ratio of the reacting calcium silicates, activation energies increase from 9.8 kcal/mole for  $\text{Ca}_3\text{SiO}_5$  to 22.9 kcal/mole for  $\beta\text{-CaSiO}_3$ .

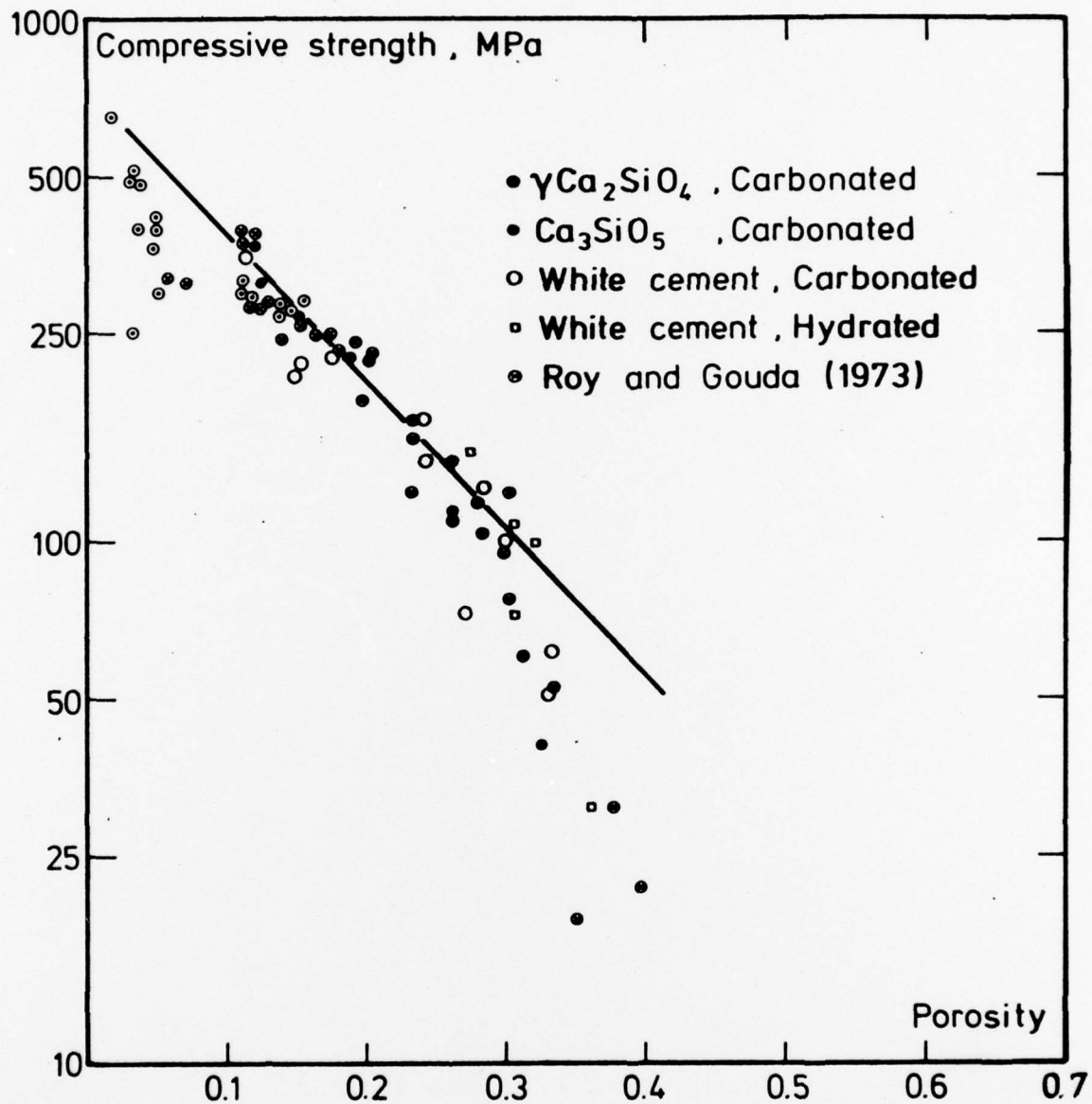


Figure 16. Relationship of compressive strength to capillary porosity of carbonated and hydrated compacted materials.

- 2) The carbonation reaction fits a diffusion controlled diminishing volume model.
- 3) The carbonation reaction rate is strongly influenced by relative humidity in that the reaction rate decreases as relative humidity decreases.
- 4) The carbonation reaction rate decreases rapidly with a decrease in  $\text{CO}_2$  partial pressure  $< 0.12$  and decrease less rapidly as  $\text{CO}_2$  partial pressures become  $> 0.12$ .
- 5) The initial rate of reaction is very sensitive to the presence of free water.
- 6) The reaction of dry powders of calcium silicates with  $\text{CO}_2$  and water vapor results in the formation of calcium carbonate and a calcium silicate hydrate with a very low Ca/Si ratio or a silica gel.
- 7) The crystalline polymorph of  $\text{CaCO}_3$  which forms during the reaction is controlled by the moisture content of the reacting material. Calcite forms if water is present, whereas aragonite forms in the absence of free water.
- 8) The Ca/Si and  $\text{H}_2\text{O}/\text{Si}$  ratios of the calcium silicate hydrate reaction product decreases with increasing degree of reaction. This is probably related to condensation (or polymerization) of the silica gel structure (i.e., further formation of Si-O-Si bonds).
- 9) The surface area of the calcium silicate hydrate (silica gel) ranges from  $400 \text{ m}^2/\text{g}$  to  $100 \text{ m}^2/\text{g}$ , decreasing with increasing degree of reaction.

- 10) The low lime calcium silicate hydrate (or silica gel) reaction product has a highly polymerized silica structure, which maintains the morphology of the original calcium silicate structure after treatment in HCl.
- 11) Reaction rates of all calcium silicates studied increased significantly with increased temperatures up to 60°C.
- 12) The size of CaCO<sub>3</sub> crystallites increased as CO<sub>2</sub> pressure was increased to 54 atm.
- 13) The calcium silicate hydrate (or silica gel) forms primarily within the grain boundaries of the original reacting calcium silicates, whereas the calcium carbonate reaction product generally forms outside of the original grain boundary.
- 14) Strength development of compacts of calcium silicate compacts carbonated for various lengths of time show a direct strength-porosity relationship, similar to that shown for hydrated hydraulic calcium silicates.
- 15) Carbonation of compacts results in the carbonation of the outer portion of the compact which impedes diffusion of CO<sub>2</sub> into the compact and slows the carbonation process.
- 16) The reaction rate of non-hydraulic calcium silicates  $\gamma$ -Ca<sub>2</sub>SiO<sub>4</sub> and CaSiO<sub>3</sub> generally increase with an increase in CO<sub>2</sub> pressure up to 54 atm.

5.0 References

1. Cements Research Progress 1974, coordinating editor J. F. Young, Am. Ceramic Soc., 234 pp., 1975.
2. Cements Research Progress 1978, coordinating editor J. F. Young, Am. Ceramic Soc., 351 pp., 1979.
3. Goodbrake, C. J., "Reaction of Beta Dicalcium Silicate and Tricalcium Silicate with Carbon Dioxide and Water," Ph.D. thesis, Dept. of Ceramic Eng. Univ. of IL., Urbana-Champaign, 135 pp., 1978.
4. Ghinazzi, J. M., "Effect of Pressure on the Reaction of Beta Calcium Silicate and Gamma Dicalcium Silicate with Carbon Dioxide and Water," M.S. thesis, Dept. of Ceramic Eng., Univ. of IL., Urbana-Champaign, 94 pp., 1979.
5. Berger, R. L., unpublished results.
6. Roy, D. M. and Gouda, G. R., "High Strength Generation in Cement Pastes," Cem. Concr. Res., 3, No. 6, 807-820, 1973.

6.0 Appendix 1

Reprint of "Reaction of Beta-Dicalcium Silicate and Tricalcium Silicate with Carbon Dioxide and Water Vapor" by C. J. Goodbrake, J. F. Young and R. L. Berger, J. American Ceramic Society, 62, No. 3-4, March-April 1979.

# Reaction of Beta-Dicalcium Silicate and Tricalcium Silicate with Carbon Dioxide and Water Vapor

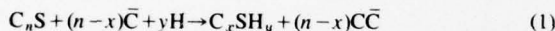
C. J. GOODBRAKE,\* J. F. YOUNG,\* and R. L. BERGER\*

Departments of Civil Engineering and Ceramic Engineering, University of Illinois at Urbana-Champaign, Urbana, Illinois 61801

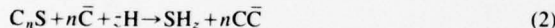
The carbonation-reaction kinetics of beta-dicalcium silicate ( $2\text{CaO}\cdot\text{SiO}_2$  or  $\beta\text{-C}_2\text{S}$ ) and tricalcium silicate ( $3\text{CaO}\cdot\text{SiO}_2$  or  $\text{C}_3\text{S}$ ) powders were determined as a function of material parameters and reaction conditions and an equation was developed which predicted the degree of reaction. The effect of relative humidity, partial pressure of  $\text{CO}_2$ , surface area, reaction temperature, and reaction time on the degree of reaction was determined. Carbonation followed a decreasing-volume, diffusion-controlled kinetic model. The activation energies for carbonation of  $\beta\text{-C}_2\text{S}$  and  $\text{C}_3\text{S}$  were 16.9 and 9.8 kcal/mol, respectively. Aragonite was the principal carbonate formed during the reaction and the rate of carbonate formation was coincident with depletion of the calcium silicates; C-S-H gel formation was minimal.

## I. Introduction

THE accelerated hydration of hydraulic calcium silicates,  $\text{C}_3\text{S}$  and  $\beta\text{-C}_2\text{S}$ , in the presence of high  $\text{CO}_2$  concentrations leads to rapid strength development of compacted mortars.<sup>1</sup> It has been suggested<sup>1,2</sup> that the carbonation process initially forms calcite and C-S-H according to:



The C-S-H which forms initially may be similar to that formed in conventional hydration but is believed to carbonate rapidly so that the final reaction products are calcite and silica gel, the overall reaction being:



During the initial carbonation of compacts the high heat evolution drives water from the specimen and the central core of the compact reacts only slightly. Subsequent carbonation of the core will occur only in the presence of water vapor. Accordingly, a study of the carbonation process under these conditions was of interest. The use of water vapor enables the reaction conditions to be well defined and is thus suitable for a detailed kinetic study.

## II. Experimental Procedure

### (1) Materials

The  $\beta\text{-C}_2\text{S}$  was synthesized in the laboratory and analyzed chemically and by X-ray diffraction (XRD). The chemical analysis is given in Table I; no other silicates were detected. Its density was

\*Presented at the 80th Annual Meeting, The American Ceramic Society, Detroit, Michigan, May 10, 1978 (Cements Division, No. 33-T-78). Received June 15, 1978; revised copy received September 7, 1978.

Based in part on a thesis submitted by C. J. Goodbrake for the Ph. D. degree in ceramic engineering, University of Illinois, April 1978.

Supported by the U.S. Army Research Office under Grant No. DAAG 29-76-G-0116.

\*Member, the American Ceramic Society.

†Now with the 3M Co., St. Paul, Minnesota 55101.

‡Within this paper, conventional cement chemistry notation is used, i.e. C = CaO, S =  $\text{SiO}_2$ , H =  $\text{H}_2\text{O}$ ,  $\bar{\text{C}}$  =  $\text{CO}_2$ .

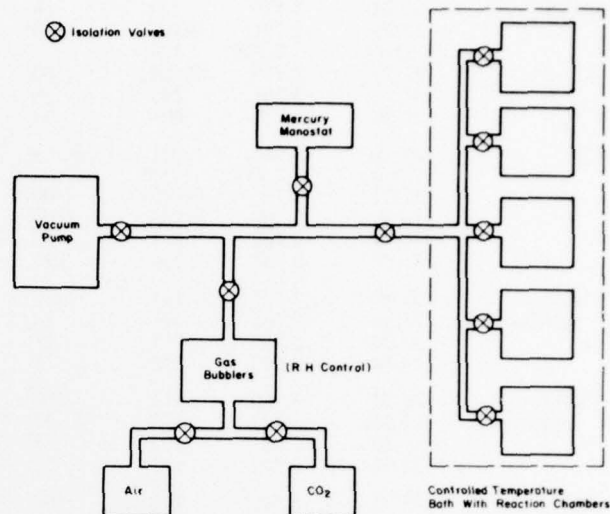


Fig. 1. Schematic view of carbonation apparatus.

$3.26 \pm 0.01 \text{ g/cm}^3$ , which compares favorably with published data. The  $\beta\text{-C}_2\text{S}$  was then ball-milled to a Blaine fineness of  $3850 \text{ cm}^2/\text{g}$  and further reduced in size by a vibratory mixer<sup>3</sup> to specific surface areas of 5300 and  $6300 \text{ cm}^2/\text{g}$ . All of the powder fractions were stored in sealed glass vials until needed. The chemical analysis of the  $\text{C}_3\text{S}$  used in this study<sup>3</sup> is also given in Table I; no other calcium silicates were detected by XRD. The  $\text{C}_3\text{S}$  was milled to a fineness of 3900, 5400, and  $6280 \text{ cm}^2/\text{g}$  using the above methods.

### (2) Carbonation

Approximately 3 g of dry powdered calcium silicate was weighed into a clean, dry, glass petri dish and placed into the carbonation-reaction vessel. Two types of reactors were used; the first consisted of a double-walled glove bag with dual seal openings and a volume of 45 L and the second consisted of five 11-L glass vacuum desiccators which were connected in parallel to a conditioned gas supply (Fig. 1).

The partial pressures of  $\text{CO}_2$  were controlled by evacuating the desiccators and backfilling to prescribed pressures (as determined by the mercury manostat). The relative humidity (rh) was controlled by bubbling the  $\text{CO}_2$  through saturated solutions of specific salts to attain the proper degree of moisture in the gas stream. Table II lists the saturated salts used for the rh conditioning. After carbonation all of the samples were dried by washing with 5 mL of acetone; the specimens were sealed in 20-mL glass vials until needed.

### (3) Analysis of Carbonated Powder

After carbonation, samples were analyzed by quantitative X-ray

§Spex Industries, Inc., Scotch Plains, N.J.  
§Portland Cement Association, Skokie, Ill.

Table I. Oxide Analyses of Calcium Silicates

| Compound                   | Amount present (wt%) |                  |   |                                |      |                   |                  |                 |      |                  |                 |
|----------------------------|----------------------|------------------|---|--------------------------------|------|-------------------|------------------|-----------------|------|------------------|-----------------|
|                            | CaO <sup>*</sup>     | SiO <sub>2</sub> | Al <sub>2</sub> O <sub>3</sub> <sup>†</sup> | Fe <sub>2</sub> O <sub>3</sub> | MgO  | Na <sub>2</sub> O | K <sub>2</sub> O | SO <sub>3</sub> | CaO  | LOI <sup>‡</sup> | IR <sup>§</sup> |
| $\text{C}_3\text{S}$       | 71.33                | 25.70            | 0.00  | 0.14                           | 0.64 | 0.01              | 0.00             | 0.05            | 0.72 | 0.76             | 0.22            |
| $\beta\text{-C}_2\text{S}$ | 64.06                | 33.28            | 0.12  | 0.10                           | 0.48 | 0.00              | 0.00             | 0.04            | 0.00 | 1.00             | 0.44            |

\*Excluding free CaO. †Includes  $\text{TiO}_2$  and  $\text{P}_2\text{O}_5$ . ‡Loss on ignition. §Insoluble residue.

**Table II. Constant Humidity Saturated Salt Solutions**

| Salt   | Rel. humidity (%) | Salt   | Rel. humidity (%) |
|--|-------------------|--|-------------------|
| H <sub>3</sub> PO <sub>4</sub> · ½H <sub>2</sub> O | 9.0               | Na <sub>2</sub> Cr <sub>2</sub> O <sub>7</sub> · 2H <sub>2</sub> O | 55.0              |
| MgCl <sub>2</sub> · 6H <sub>2</sub> O              | 33.0              | NH <sub>4</sub> Cl   | 79.5              |

**Table III. Diffraction Peaks Used in QXDA**

| Phase                            | 2θ value | d (Å)  | Diffracting plane |                  |
|----------------------------------|----------|--------|-------------------|------------------|
|                                  |          |        | (hkl)             | l/l <sub>0</sub> |
| β-C <sub>2</sub> S               | 31.04    | 2.879  | 121               | 8                |
|                                  | 32.00    | 2.794  | D(104)            | (100)            |
|                                  | 32.11    | 2.785* | 122               |                  |
|                                  | 32.56    | 2.748  | D(202)            | (100)            |
|                                  | 34.35    | 2.608  | 212               | 20               |
|                                  | 41.20    | 2.189  | 031               | 21               |
| C <sub>3</sub> S                 | 29.53    | 3.022  | 021               | (44, 13)         |
|                                  | 30.20    | 2.957* | 202               |                  |
|                                  | 32.22    | 2.776  | D(009)            | (100)            |
|                                  | 32.77    | 2.730  | D(024)            | (100)            |
|                                  | 34.44    | 2.602  | 205               | 52               |
|                                  | 41.28    | 2.185  | 208               | 33               |
| CaCO <sub>3</sub><br>(calcite)   | 29.40    | 3.035  | 104               | 100              |
|                                  | 35.96    | 2.495  | 110               | 14               |
|                                  | 39.40    | 2.285  | 113               | 18               |
|                                  | 43.14    | 2.095  | 202               | 18               |
| CaCO <sub>3</sub><br>(aragonite) | 26.24    | 3.396  | 111               | 100              |
|                                  | 27.25    | 3.273  | 021               | 52               |
|                                  | 36.20    | 2.481  | 200               | 33               |
|                                  | 37.93    | 2.372  | 112               | 38               |
| TiO <sub>2</sub><br>(anatase)    | 25.35    | 3.510  | 101               | 100              |
|                                  | 37.78    | 2.379  | 004               | 22               |
|                                  | 48.07    | 1.891  | 200               | 33               |

\*Total area of doublets was used for reference peak.

diffraction analysis (QXDA) using TiO<sub>2</sub> (anatase, 25 wt%) as an internal standard. A diffractometer\* with CuK α radiation was used to record diffraction patterns at a scanning speed of ¼° to ½° 2θ/min. Five separate peaks were used for each silicate (Table III) and each sample was run in triplicate, using a fresh packing for each run. The degree of reaction, as determined by the amount of unreacted silicate, could be estimated to ±3 wt%. The amount of calcium carbonate was similarly determined.

When samples had a low degree of reaction (short periods of carbonation) an external standard method was more satisfactory. For very high degrees of reaction (long periods of carbonation) the degree of carbonation was calculated from the amount of CC formed based on Eq. (2). The internal standard method was used for 10 to 90% of total reaction.

The degree of carbonate formation was also determined by constant-temperature pyrolysis techniques. The carbonated sample was dried at 105°C to constant weight to remove uncombined water, then heated to 350°C for 4 h; the weight difference between 105° and 350°C was due to combined water. The sample was then heated to 1000°C; the weight difference between 350° and 1000°C was due to decomposition of carbonate and was equal to the weight of CO<sub>2</sub>. The weight of carbonate could be calculated and compared to QXDA values.

The polymorph of calcium carbonate (calcite or aragonite) was identified by XRD. Morphology was studied by scanning electron microscopy<sup>†</sup> using samples that were sputter-coated with gold. The powders were mounted on specimen studs using silver conducting paint containing a little Duco<sup>‡</sup> cement.

### III. Results and Discussion

#### (1) Kinetics and Stoichiometry

Figure 2 shows the behavior of dry β-C<sub>2</sub>S and C<sub>3</sub>S powders

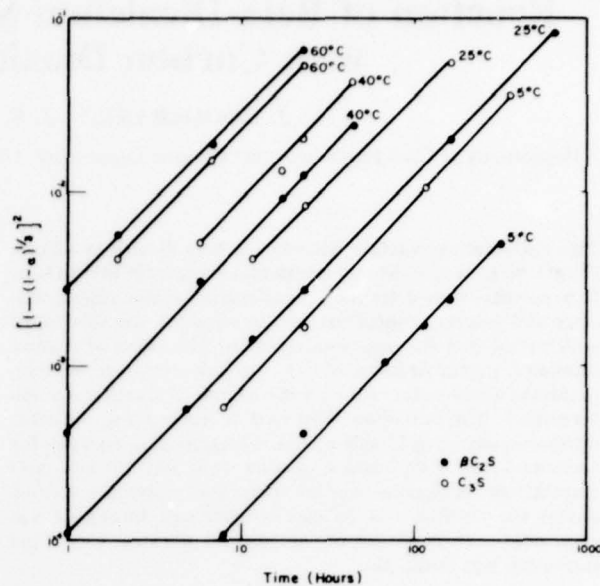


Fig. 2. Diffusion-controlled decreasing-volume kinetic model for carbonating β-C<sub>2</sub>S and C<sub>3</sub>S powders (3900 cm<sup>2</sup>/g).

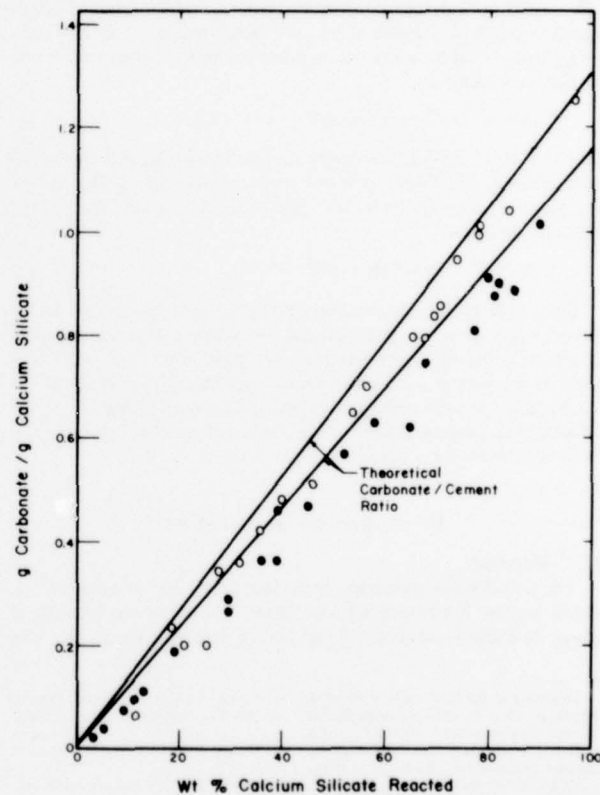


Fig. 3. Calcium carbonate formation vs degree of carbonation (100% rh, 1.0 atm CO<sub>2</sub>, 25°C).

reacted at 5°, 25°, 40°, and 60°C. When  $\log [1 - (1 - \alpha)^{1/3}]^2$  is plotted against  $\log t$  the plots are nearly linear and the slopes are  $\approx 1.0$ , indicating a diffusionally controlled reaction. C<sub>3</sub>S powders reacted to a greater degree than β-C<sub>2</sub>S for all temperatures except 60°C. The degree of carbonation was difficult to determine for samples which were <10 wt% reacted.

Figure 3 shows the amount of carbonate formed per gram of anhydrous calcium silicate reacted. Both β-C<sub>2</sub>S and C<sub>3</sub>S form

\*Norelco, North American Philips Co., New York, N.Y.

†Model JSM-U3, JEOLCO, Inc., Medford, Mass.

‡E. I. du Pont de Nemours & Co., Inc., Wilmington, Del.

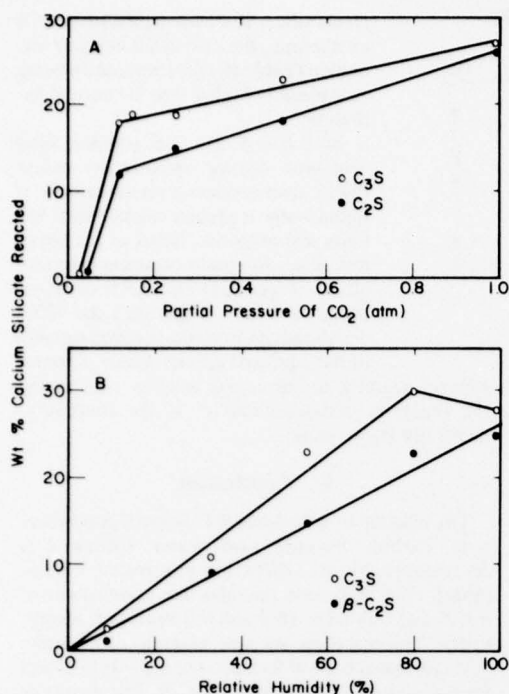


Fig. 4. Effect of (A) relative humidity and (B)  $\text{CO}_2$  partial pressure on kinetics of carbonation (at  $40^\circ\text{C}$  for 24 h).

carbonate at the same rate as the silicate is depleted, according to Eq. (2). The slight negative deviation of the experimental data from the theoretical carbonate line indicates that a small amount of C-S-H was formed, as in Eq. (1).

### (2) Effect of Experimental Parameters

The rh of the  $\text{CO}_2$  above that of the dry calcium silicate partially controls the degree of carbonation which, at 24 h with  $P_{\text{CO}_2} = 1.0$  atm, increased with increasing rh in an approximately linear manner (Fig. 4(B)). Since water is essential for carbonation to occur and since water vapor in the  $\text{CO}_2$  is the only source of water, the positive influence of rh was expected. There appears to be a slight decrease in the degree of reaction at 100% rh, which may be due to the formation of a liquid water film which serves as a diffusion barrier for water and  $\text{CO}_2$ . Similar results were reported by Verbeck<sup>3</sup> on wetted portland cement carbonated in varying rh conditions.

Figure 4(A) shows the effect of  $P_{\text{CO}_2}$  on the degree of carbonation. A threshold value exists for both  $\beta\text{-C}_2\text{S}$  and  $\text{C}_3\text{S}$  at  $\approx 0.025$  atm  $\text{CO}_2$ . Below this value carbonation was not detectable at 24 h, although carbonation has been observed after prolonged exposure to atmospheric concentrations of  $\text{CO}_2$  (0.0003 atm by volume). The criteria for carbonation, therefore, are the concentration of  $\text{CO}_2$  and the reaction time. The effect of  $P_{\text{CO}_2}$  was most pronounced between 0.025 and 0.12 atm, whereas at higher partial pressures it was much less. The apparent break in the carbonation curves at 0.12 for both  $\beta\text{-C}_2\text{S}$  and  $\text{C}_3\text{S}$  is caused by a saturation limit of  $\text{CO}_2$  in the adsorbed water on the dry silicate grains at the reaction conditions indicated in Fig. 4(A).

### (3) Carbonation Kinetics

Both  $\beta\text{-C}_2\text{S}$  and  $\text{C}_3\text{S}$  powders follow a decreasing-volume, diffusion-controlled kinetic model<sup>4</sup> which is expressed by:

$$[1 - (1 - \alpha)^{1/3}]^2 = K_T' t \quad (3)$$

where  $\alpha$  = degree of carbonation,  $K_T'$  = apparent rate constant, and  $t$  = time of reaction.  $K_T'$  depends on several material properties, as shown by

$$K_T' = \frac{KD/r}{r_0^2} = KA^2 \quad (4)$$

where  $K$  = actual rate constant,  $D$  = diffusion coefficient,  $r_0$  = aver-

Table IV. Reaction Parameters for Carbonation

| Compound                   | $K_0'$ ( $\text{h}^{-1}$ ) | $E_a$ (kcal/mol) | $\Delta H_f$ (kcal/mol) |
|----------------------------|----------------------------|------------------|-------------------------|
| $\text{C}_3\text{S}$       | $3.44 \times 10^4$         | 9.8              | -83                     |
| $\beta\text{-C}_2\text{S}$ | $2.39 \times 10^9$         | 16.9             | -44                     |

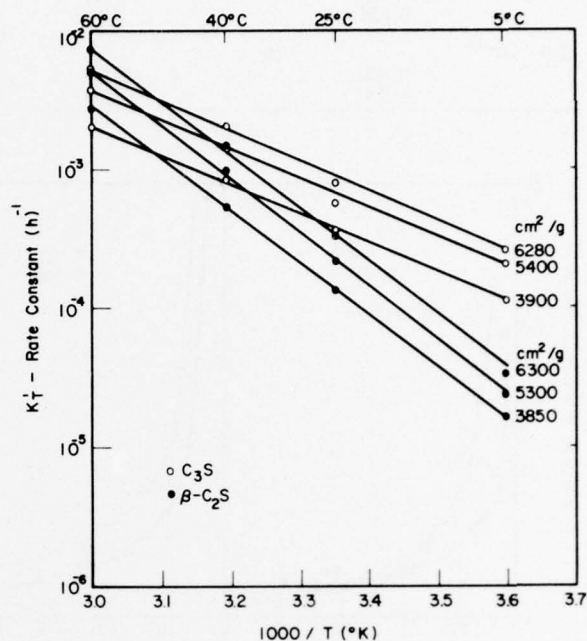


Fig. 5. Arrhenius plots for carbonation of  $\text{C}_3\text{S}$  and  $\beta\text{-C}_2\text{S}$ .

age particle size, and  $A$  = average surface area. The temperature dependency is given by the Arrhenius equation:

$$K_T' = K_0 \exp(-E_a/RT) \quad (5)$$

Where  $K_0$  = preexponential term,  $E_a$  = activation energy,  $R$  = gas constant, and  $T$  = temperature ( $^\circ\text{K}$ ). Combining Eqs. 3 to 5 gives

$$\alpha = 1 - \{1 - [K_0' \exp(-E_a/RT) A^2 t]^{1/2}\}^3 \quad (6)$$

where  $K_0' = K_0 D$ . The values for the reaction parameters  $K_0'$  and  $E_a$  are given in Table IV.

### (4) Prediction of $\alpha$

Equation 6 can be used to calculate  $\alpha$  for powders of varying surface area reacted at different temperatures. The constants for Eq. (6) were obtained from Fig. 5, which shows the Arrhenius plots for  $\beta\text{-C}_2\text{S}$  and  $\text{C}_3\text{S}$ . Cross plots of the apparent rate constant  $K_T'$  show the linear dependence of  $A^2$  and  $\alpha$ . The calculated values from Eq. (6) were accurate to  $\pm 3$  wt% over many reaction temperatures and particle finenesses. Equation (6) was developed using fixed reaction conditions of 1.0 atm  $\text{CO}_2$  and 100% rh. The reaction at other  $P_{\text{CO}_2}$  and rh values can be determined by multiplying Eq. (6) by the following constants, which were determined from Fig. 4:

$$\alpha_{rh} = (\alpha)[(M \times \% rh) + C] / (T/313) \quad (7)$$

$$\alpha_{P_{\text{CO}_2}} = (\alpha)[(L \times P_{\text{CO}_2}) + B] / 313/T \quad (8)$$

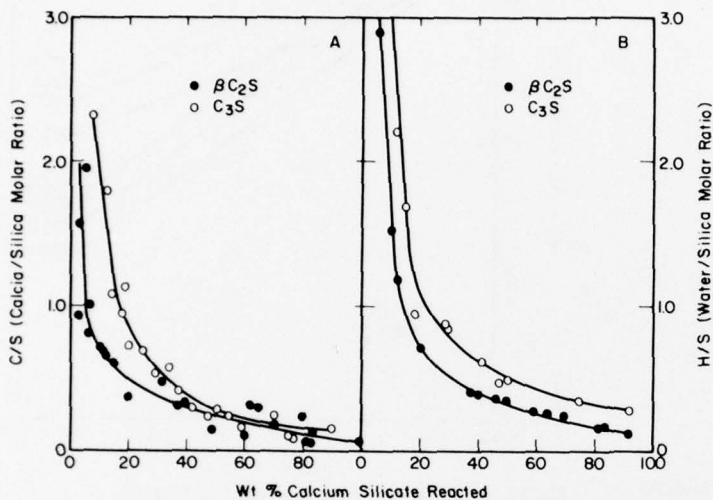
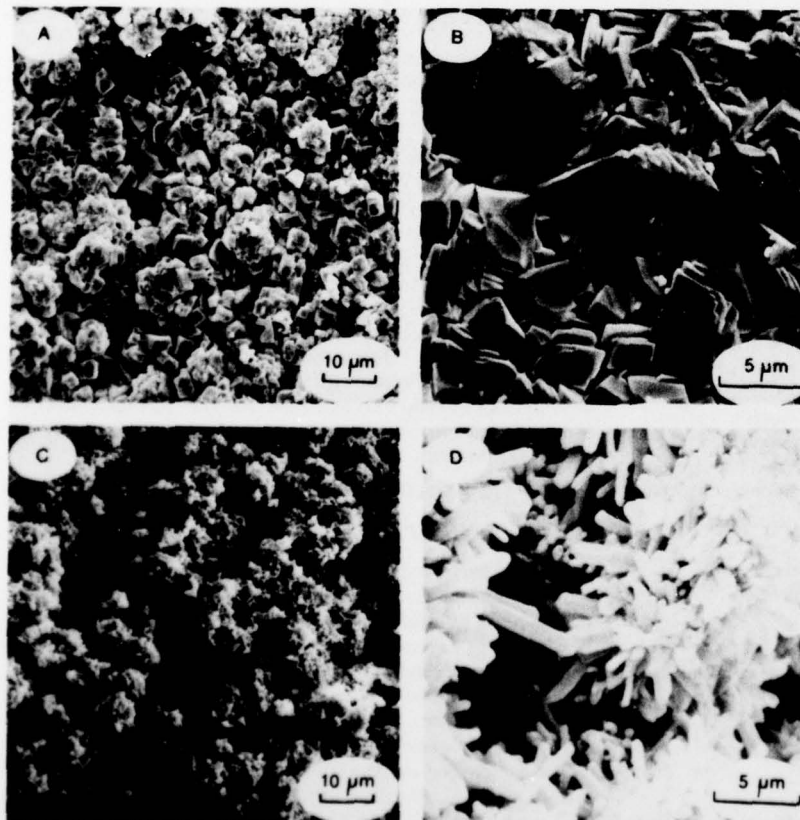
The correct curve-fitted coefficients for Eqs. (7) and (8) are listed in Table V.  $T$  is the reaction temperature (in  $^\circ\text{K}$ ) and these equations thus indicate a linear dependency of rh and  $P_{\text{CO}_2}$  with temperature ( $P_{\text{CO}_2}$  being an inverse dependence). Although the temperature dependence of rh and  $P_{\text{CO}_2}$  should actually be curvilinear functions, the linear correlation is a good approximation in the temperature range studied.

### (5) Reaction Stoichiometry

The carbonation mechanism for anhydrous powders is best described by Eq. (2). Analyses indicate that a small amount of C-S-H forms, which rapidly loses CaO and water (Fig. 6) to form amor-

**Table V.** Effect of Experimental Variable on Carbonation Parameters That Modify Eq.(6)

| M                     | L     | C      | B      | Range                 | Eq. |
|-----------------------|-------|--------|--------|-----------------------|-----|
| 0                     |       | 0-0.29 | $C_3S$ | 80-100% rh            | 7   |
| $3.63 \times 10^{-3}$ |       | 0      |        | 0-80% rh              | 7   |
|                       | 1.263 |        | -0.20  | $0.025-0.12 P_{CO_2}$ | 8   |
|                       | 0.125 |        | 0.16   | $0.12-1.0 P_{CO_2}$   | 8   |
| $2.6 \times 10^{-3}$  |       | 0      | $C_2S$ | 0-100% rh             | 7   |
|                       | 1.43  |        | -0.06  | $0.05-0.12 P_{CO_2}$  | 8   |
|                       | 0.18  |        | 0.10   | $0.12-1.0 P_{CO_2}$   | 8   |

**Fig. 6.** Composition of C-S-H formed during carbonation in terms of (A) C/S ratios and (B) H/S ratios.

phous silica. The carbonation reaction is exothermic, the calculated heats of formation (Table III) for carbonation being considerably higher than for normal hydration.<sup>4</sup>

Both  $\beta$ - $C_2S$  and  $C_3S$  powders form aragonite during carbonation unless liquid water condenses on the sample. If liquid water is present calcite forms initially and aragonite forms as the specimen dries. Aragonite occurs as prismatic blocks (Figs. 7(A) and 7(B)) or as orthorhombic laths (Figs. 7(C) and 7(D)) which radiate from the original surfaces of the equiaxed silicate grains. Conversion of aragonite to calcite was not observed during the reaction, although calcite is the thermodynamically stable phase.

### V. Conclusions

The reaction of anhydrous  $\beta$ - $C_2S$  and  $C_3S$  powders with carbon dioxide and water followed a decreasing-volume, diffusion-controlled kinetic model. The activation energies for carbonation of  $\beta$ - $C_2S$  and  $C_3S$  were 16.9 and 9.8 kcal/mol, respectively. The reactions are also strongly exothermic, with calculated heats of formation being -44 kcal/mol for  $\beta$ - $C_2S$  and -83 kcal/mol for  $C_3S$ . The degree of carbonation increased with increased reaction temperature, particle-surface area, reaction time, relative humidity, and partial pressure of  $CO_2$ . Carbonation of anhydrous  $\beta$ - $C_2S$  and  $C_3S$  formed aragonite and silica gel. Small quantities of C-S-H gel were formed in the initial stages of the reaction.

### References

- 1 J. F. Young, R. L. Berger, and J. Breese, "Accelerated Curing of Compacted Calcium Silicate Mortars on Exposure to  $CO_2$ ," *J. Am. Ceram. Soc.*, **57**[9] 394-97 (1974).
- 2 R. L. Berger, J. F. Young, and K. Leung, "Acceleration of Hydration of Calcium Silicates by Carbon Dioxide Treatment," *Nature (London), Phys. Sci.*, **240**[97] 16-18 (1972).
- 3 G. Verbeck, "Carbonation of Hydrated Portland Cement," *Am. Soc. Test. Mater., Spec. Tech. Publ.*, **1958**, No. 205, pp. 17-36.
- 4 R. Kondo and S. Ueda, pp. 203-48 in Proceedings of the 5th International Symposium on the Chemistry of Cement, Part II, Vol. II, Cement Association of Japan, Tokyo, 1969.

**Fig. 7.** Characteristic morphologies of aragonite formed during carbonation. (A) and (B) Prismatic blocks ( $\beta$ - $C_2S$ , 22 days at 25°C); (C) and (D) orthorhombic laths ( $C_3S$ , 3 days at 60°C).

## 7.0 Participating Scientific Personnel

R. Lee Berger, Professor Civil and Ceramic Engineering

J. Francis Young, Professor Civil and Ceramic Engineering

Cris J. Goodbrake\*, Ph.D. candidate, Ceramic Engineering

John M. Ghinazzi\*\*, M.S. candidate, Ceramic Engineering

Wilhelm Hansen, Ph.D. candidate, Civil Engineering

\*received Ph.D. in Ceramic Engineering while employed on project.

\*\*received M.S. in Ceramic Engineering while employed on project.

## 8.0 Publications

1. Goodbrake, C. J., Young, J. F. and Berger, R. L., "Reaction of Beta-Dicalcium Silicate and Tricalcium Silicate with Carbon Dioxide and Water Vapor," J. Am. Ceramic Soc., 62, No. 3-4, p. 168-171, 1979.
2. Goodbrake, C. J., Young, J. F. and Berger, R. L., "Reaction of Hydraulic Calcium Silicates with Carbon Dioxide and Water," J. Am. Ceramic Soc., 62, No. 7-8, 1979.
3. Berger, R. L., "Stabilization of Silicate Structures by Carbonation," Cem. Concr. Res., 9, 5, p. 649-652, 1979.
4. Goodbrake, C. J., "Reaction of Beta Dicalcium Silicate and Tricalcium Silicate with Carbon Dioxide and Water," Ph.D. thesis, Dept. of Ceramic Eng. Univ. of IL., Urbana-Champaign, 135 pp., 1978.
5. Ghinazzi, J. M., "Effect of Pressure on the Reaction of Beta Calcium Silicate and Gamma Dicalcium Silicate with Carbon Dioxide and Water," M.S. thesis, Dept. of Ceramic Eng., Univ. of IL., Urbana-Champaign, 94 pp., 1979.